Copy
RM L56J31

RESEARCH MEMORANDUM

BASIC PERFORMANCE CHARACTERISTICS OF SEVERAL SUBSONIC-DIFFUSER—BYPASS-DUCT COMBINATIONS FOR USE WITH SUPERSONIC INLETS

By Charles C. Wood

Langley Aeronautical Laboratory
Langley Field, Va.

NATIONAL ADVISORY COMMITTEE
FOR AERONAUTICS

WASHINGTON

January 21, 1957

NACA RM L56J31

NATIONAL ADVISORY COMMITTEE FOR AERONAUTICS

RESEARCH MEMORANDUM

BASIC PERFORMANCE CHARACTERISTICS OF SEVERAL SUBSONIC-DIFFUSER—BYPASS-DUCT COMBINATIONS FOR USE WITH SUPERSONIC INLETS

By Charles C. Wood

SUMMARY

In connection with the problem of matching inlet and engine air flows, the basic performance characteristics of several types of designs of subsonic-diffuser—bypass-duct combinations were determined for bypass flows up to one-third of the total flow. The models were of the directly connected type wherein the desired boundary-layer condition upstream from the bypass was obtained by controlling the Mach number of the shock downstream from the diffuser throat. It was found that a bypass-duct design procedure, whereby a hole is cut in one side wall of a diffuser and a scoop inserted, is greatly oversimplified and that satisfactory performance cannot be obtained because of the extreme adverse pressure gradient downstream from the scoop established by sudden removal of relatively large quantities of air combined with the diverging wall on the downstream face of the scoop. A bypass arrangement designed to produce at maximum bypass flow a minimum of adverse pressure gradient between the scoop lip and the engine face station produced substantially better performance. The performance for such a design was found to be satisfactory for the various inlet boundary-layer conditions examined.

INTRODUCTION

The thrust and general operation of turbojet propulsion systems are directly dependent on the performance of the inlet and associated ducting. The performance or relative efficiency of such duct systems is usually gaged by the drag, pressure recovery, uniformity of the exit velocity distribution, and stability of the flow. A current problem in the design of internal-flow systems which significantly affects these performance indices is that of matching the inlet and compressor air flows. One solution to this problem is the use of a bypass duct. The inlet is sized for the maximum required engine air flow, and for operating conditions

where surplus air flow is taken in by the inlet, the excess is bypassed around the engine and discharged elsewhere. This procedure permits high pressure recovery and low drag by maintaining a normal shock position just downstream from the minimum area section.

Data on the bypass subject are available in references 1 to 4. References 1 to 3 contain total-pressure loss and drag data on complete inlet—bypass-duct configurations. The models were conical spike-type supersonic inlets which differed in design principally in the direction of discharge of the bypass air and in the circumferential location of the bypass. Conclusions from these investigations, for which flow was removed through either one or two limited area sectors located upstream from the diffuser exit, are that significant drag reductions relative to other matching techniques are possible without reducing the total pressure recovery. Detail design of the ducts in the region where the air-flow division occurs was not considered. Reference 4 is a preliminary report on part of the data contained herein. Additional information on total-pressure losses in branch ducts is available in reference 5.

The purpose of the present report is to present comprehensive data showing the effects on both total-pressure loss and diffuser exit velocity distribution resulting from bypassing air flow from a subsonic diffuser. Other factors of interest to be treated herein concern the effects on bypass diffuser performance of shock—boundary-layer interaction and the establishment of the basic performance characteristics of several general types of bypass-duct designs. All data are from directly connected duct tests with some important effects of supersonic inlet operation obtained by operation with a standing normal shock in the subsonic diffuser. Up to 35 percent of the total flow was bypassed from one of the side walls near the diffuser exit. Maximum Mach number in the plane of the bypass was 0.55. The corresponding Reynolds number based on the hydraulic diameter was 1.97×10^6.

SYMBOLS

H	total pressure
p	static pressure
M	mean Mach number (see section entitled "Performance Parameters")
M_s	Mach number of the flow in the diffuser at which the shock occurs
u	local stream velocity

U maximum velocity in a velocity distribution at a given duct station

x distance from the diffuser wall opposite the bypass side

w duct width in the same plane as dimension x

ΔP pressure difference between a specific wall orifice and a wall orifice at station 1a

A bar over a symbol indicates that the quantity is mass weighted.

Subscripts:

0 reference station at inlet bell

1a, 1b survey stations upstream from bypass location

2, 2a, 2b survey stations at locations corresponding to engine face station

3 survey station for total-pressure recovery of engine air flow

4 survey station for total-pressure recovery of bypass air flow

APPARATUS

Test Equipment

A diagram of the test setup is shown in figure 1. Air flow from a blower passed into a 30-inch-diameter duct, an inlet bell, and the diffuser model, where it was divided into two streams (the engine air stream and the bypass stream). Venturi meters (stations 3 and 4) followed by discharge diffusers were located at the end of the engine air and bypass ducts.

Diffuser model I was simply a conventional straight-walled diffuser with a low expansion angle and with the bypass scoop mounted on one side wall near the diffuser exit. The diffuser cross section was rectangular at the inlet, and the top and bottom walls were parallel. The side walls each diverged at an angle of 3.1° to produce between stations 0 and 2 an area ratio of 2.0:1. Interception of the bypass-duct center line with the diffuser center line occurred at a 30° angle at a point 61 percent of the total diffuser length from the diffuser throat. The bypass-duct height and width were constant, and the bypass-duct height was equal to the diffuser height.

Four different scoop extensions were tested (fig. 2) varying from the flush type (number 1) to the type (number 4) extending a sufficient distance to intercept approximately one-third of the diffuser flow at an inlet velocity ratio of 1. Scoops number 2 and 3 intercepted in a similar manner 10 and 20 percent of the flow, respectively.

Efforts were made to improve the diffuser flow of model I by the use of various flow control devices; a typical configuration is shown in figure 3. This configuration consists of two sheet-metal vanes located in the immediate vicinity of the scoop (number 2) and four vortex generators located $12\frac{1}{4}$ inches upstream and on the divergent wall opposite the scoop side. This configuration, performancewise, was the best of three which were tested. Vane spacing was the only variable.

Drawings of a second model tested (model II) are shown in figure 4. Model II was obtained by altering model I and differs in the following respects:

(1) Two interchangeable duct sections were located downstream from the inlet bell in order to provide different minimum areas and, consequently, two nominal Mach number levels at station 2b of 0.4 and 0.7 for models IIa and IIb, respectively. These Mach numbers bracket current operating Mach numbers for turbojet compressors.

(2) The ducting was altered downstream from the scoop leading edge so that (a) the diffuser exit, station 1b, (station 2 for model I) was located just upstream from the scoop lip and the diffuser exit area included the scoop inlet area, thus producing a splitter-type configuration; and (b) the engine air duct contracted slightly downstream from the scoop leading edge instead of expanding rapidly as for model I.

Proportions of models I, IIa, and IIb may be compared in figure 5, which consists of scale drawings of the three models. The diffuser exit area for models IIa and IIb was about 50 percent of that for model I.

Instrumentation

Wall static orifices were located along the diffuser wall opposite the bypass side, and at the midpoints of the top, bottom, and two side walls at stations 0, 1b, 3, and 4 (figs. 1 and 4). The reference total pressure and temperature were measured in the 30-inch duct upstream of the inlet bell. Total-pressure traverses from each wall were made at station 1b for the purpose of calibrating flow conditions immediately upstream from the bypass. These survey tubes were removed for downstream surveys. Similar measurements were made at station 3 to determine the engine duct recovery. A single total-pressure traverse on the horizontal

center line at station 2 for model I and stations 2a and 2b for models IIa and IIb was made to obtain flow distributions. Three total-pressure traverses were made across the narrow dimension of the duct at station 4 to obtain bypass-duct recovery. All survey data were recorded by using commercial transducer pressure cells in conjunction with electronic data plotters which limited the frequency response to 10 cycles or less and gave a continuous plot of the pressure. Data in all cases were obtained to within 0.05 inch of each wall.

TEST PROCEDURE AND BASIS OF DATA COMPARISON

Test Procedure

Total-pressure surveys at station 1b were made for the purpose of calibrating pressure recovery and flow distribution at station 1b with the diffuser inlet choked and shocks in the diffuser in the Mach number range from 1.0 to 1.6. For these tests, the scoops were removed and the bypass duct closed and faired smooth. Similar measurements were obtained with various spoiler configurations upstream. With a normal shock of sufficient strength standing in the diffuser, the flow separated naturally, from one or the other of the diverging walls. Furthermore, for a given configuration the separation always occurred on the same wall. This result may have been due to small construction inaccuracies. Inasmuch as the configurations under investigation were asymmetrical because the bypass was on one side wall, in certain instances it was desirable to force separation on the wall opposite to that chosen naturally by the flow. Spoilers located downstream of a standing normal shock were used in these instances to fix the separation. After completing the calibration at station 1b, the survey rakes were moved to downstream stations and similar measurements performed to obtain basic pressure recoveries and flow distributions without the bypass scoops in place. Scoops were then inserted and tests made while bypassing air. Butterfly valves (figs. 1 and 4) were used to regulate the flow and permitted testing at a constant reference total pressure.

Performance Parameters

Parameters of interest in this investigation are exit-velocity distributions, total-pressure loss in both the engine air and bypass ducts, exit total-pressure distortions, longitudinal-wall static-pressure distributions, bypass air flow, and Mach number. Velocity distributions of most interest are those at the diffuser exit which would correspond to the compressor inlet, station 2 for model I, and station 2a or 2b for model II. Surveys were obtained at two exit stations for model II to evaluate the effect of a constant area duct at the exit. Distributions

are presented as the ratio of local velocity to maximum velocity. Total-pressure-loss data are presented as a coefficient $\frac{\overline{\Delta H}}{\overline{H}_{1b}}$ which is the ratio of the difference in mass-weighted total pressure between station 1b and some downstream station to the mass-weighted total pressure at station 1b. It is possible to obtain negative values of this coefficient for either the engine air or the bypass ducts under certain conditions but not in both simultaneously. A negative value may occur when a disproportionate share of high-energy air at station 1b passes through either the bypass or the engine air duct. Total-pressure-loss data are also presented as a coefficient $\frac{\overline{\Delta H}_{1b-3,4}}{\overline{H}_{1b}}$ which is obtained by mass weighting the engine air- and bypass-duct-loss coefficients. This coefficient should be positive; otherwise an increase in total pressure is indicated. The total-pressure distortion factor is the ratio of the difference between the maximum and minimum total pressure for a given distribution at station 2, 2a, or 2b to the mass-weighted total pressure $\left(\frac{H_{2,max} - H_{2,min}}{\overline{H}_3}\right)$ at station 3. In determining this factor, 5 percent of the cross-sectional area adjacent to the two side walls was ignored in order to allow for a nominal boundary-layer thickness. Static pressure distributions are presented as a coefficient $\frac{\Delta P}{\overline{H}_{1b} - P_{1a}}$ which is the ratio of the difference in pressure between a wall orifice at stations downstream of station 1a and the wall orifice at station 1a to the difference between the mass-weighted total pressure at station 1b and the static pressure at station 1a. Bypass air flow is expressed as a ratio of the mass flow through the bypass duct as determined from surveys at station 4 to the total air flow passing through the diffuser throat as determined from the inlet bell. Mean Mach numbers presented herein were determined from a one-dimensional relationship utilizing the mass flow, duct cross-sectional area, the total temperature, and the static pressure of the flow.

RESULTS AND DISCUSSION

Model I Results

Inlet conditions.- Velocity profiles at station 1b are presented in figure 6 for three different operating conditions intended to simulate both on and off design inlet operation. Measurements presented were in the midplane of the diverging side walls and perpendicular to the vertical plane through the model center. Boundary-layer condition 1 was established by choking the diffuser throat and possessed the following

characteristics: symmetrical flow, a boundary-layer thickness at each wall equal to 20 percent of the diffuser width, velocity ratios of 0.4 in proximity of the walls, values of M_{1b} and M_2 of 0.39 and 0.31, respectively. Boundary-layer condition 2 was established by choking the diffuser throat and establishing a shock in the diffuser at a Mach number of 1.43. Boundary layer 2 possessed the following characteristics: a badly distorted velocity distribution with zero flow in a region extending over 10 percent of the duct area adjacent to the wall opposite the bypass, thin boundary layer and high velocity air in proximity of the bypass wall, M_{1b} and M_2 values of 0.55 and 0.40, respectively, and significantly higher local Mach numbers than M_{1b} near the diffuser center at station 1b. Boundary-layer condition 3 was practically a reflection of boundary-layer condition 2. The switch in flow was induced by mounting a spoiler on the bypass wall. Station 1b velocity profiles made perpendicular to the parallel walls of the diffuser were symmetrical for the three boundary-layer conditions tested and velocity ratios immediately adjacent to the walls were 0.5 or greater.

Longitudinal wall static-pressure distribution.- Static-pressure distributions are presented in figure 7 for boundary-layer condition 1. The static-pressure rise between stations 1a and 2 obtained with the flush scoop and the theoretical rise as determined by one-dimensional relations are presented in figure 8 as a function of percent of total air flow bypassed. The basic condition with scoop removed and bypass opening sealed produced a static-pressure rise coefficient of about 0.4 between station 1a and station 2. (See fig. 7.) This value is about 89 percent of the ideal pressure rise indicated in figure 8 and is typical for diffusers of this area ratio, expansion rate, and inlet distribution. The blockage effects resulting from the presence of the scoops are indicated by the reductions in pressure rise in figure 7 and depend on the amount of flow bypassed and the scoop projection. The extreme condition in this respect was obtained with scoop 4, which choked the flow with no bypass flow (data not shown). At design bypass flow (32 percent) blockage effects were minimized and the pressure rise was about the same as for the basic condition, yet the ideal pressure rise is 65 percent greater than for the 0-percent bypass condition. Bypassing air flow from a diffuser subjects the downstream diffuser section to additional adverse pressure gradients, the magnitude of such pressure gradients depending upon the percentage of the flow bypassed.

Exit velocity distributions and total-pressure distortions.- Station 2 velocity distributions and total-pressure distortions are present in figures 9 and 10, respectively. For boundary-layer condition 1 the model with scoop removed and opening sealed produced at station 2 a velocity distribution almost identical to the distribution at station 1b (fig. 6) indicating the pressure rise between stations 1b and 2 noted in figure 7 had little effect on the relative size of the boundary layer. The

distribution for the flush scoop and no bypass flow is relatively uniform; however, flow does not exist in proximity of the bypass wall. Progressive increases in flow distortion occur on the scoop side with increasing scoop extension and no bypass flow, probably due to the increasing angle of attack at the scoop leading edge and high diffusion angles on the back side of the scoop. For intermediate bypass flows (18 percent) low-energy air on the bypass side is removed, and high angle of attack at the scoop lip is relieved; thus, no velocity deficiency exists on the scoop side except for scoop 4. Scoops 1, 2, and 3 have large deficiency regions on the opposite wall resulting from large adverse pressure gradients set up by bypassing flow as noted in figure 8. For approximately 31-percent bypass flow, distributions for the four scoops are practically identical; regions of velocity deficiency are on the diffuser wall opposite the bypass and occupy about one-half the duct area. Practically no flow exists adjacent to the wall. It is to be concluded for this type of configuration that uniform and acceptable distributions cannot be obtained for the bypass-flow range desired because of the blockage effects from projected scoops and the high adverse pressure gradients set up by bypassing flow. Profiles obtained with boundary layers 2 and 3 show similar trends as profiles obtained with boundary layer 1 but, in general, are somewhat more distorted.

For boundary-layer condition 1, total-pressure distortions (fig. 10) produced by scoop 4 were extremely high at low bypass flows due to the high blockage effect and resulting poor velocity distribution. Distortions for the other scoops are fairly small (about 7 to 10 percent); these smaller distortions are due to superior velocity distributions as well as lower Mach number levels. Distortions for boundary layers 2 and 3 are larger (about 15 to 27 percent) than for boundary layer 1, due to less uniform velocity distributions and higher Mach number levels.

Total-pressure loss.- Total-pressure-loss data are shown in figures 11 to 13. Losses in the engine air duct (fig. 11) indicate, for inlet boundary-layer condition 1, that scoops which projected the greatest distances into the diffuser produced the highest losses, scoop 4 producing about 20-percent loss with no bypass flow and scoops 1 and 2 only about 1- to 2-percent loss. The basic diffuser loss with no scoop and the bypass opening sealed was about 1 percent. The adverse effects of increasing amounts of bypassed flow on performance (noted in fig. 9 for station 2 velocity distributions) are not particularly noticeable because the act of bypassing the boundary layer or low-energy part of the flow at station 1b in effect increases the mean total pressure of the air entering the engine air duct $\left(\text{an effect not accounted for by } \frac{\overline{\Delta H}_{1b-3}}{\overline{H}_{1b}}\right)$. In addition, as the bypass flow increases the engine-duct dynamic pressure decreases, thus tending to reduce the absolute losses. Higher losses were observed for

boundary-layer conditions 2 and 3 than for boundary layer 1 as would be expected from the higher basic loss values. Trends with increasing bypass flow were affected by the location of the retarded velocity region at station 1b. For instance, for boundary layer 3 the total-pressure deficiency was on the bypass side; therefore, increasing the bypass flow raised $\overline{H}_3$.

Total-pressure-loss data in the bypass duct (fig. 12) show that for a given scoop the losses $\left(\text{indicated by } \frac{\overline{\Delta H}_{1b-4}}{\overline{H}_{1b}}\right)$ are entirely dependent on the total pressure of the air entering the bypass duct; thus, bypass-duct losses are influenced by the following factors in the manner noted: (1) The losses $\left(\overline{H}_{1b} - \overline{H}_4\right)$ decrease with increasing bypass flow because the proportion of air taken from the higher energy part of the boundary layer is increasing; (2) the losses decrease with increasing bypass flow because the adverse pressure gradient upstream from the scoop decreases as bypass flow approaches the design value; (3) the losses increase with increasing total-pressure distortion of the flow at station 1b. Ram recovery was observed to improve as the scoop extension was increased, especially for distorted upstream-flow distributions.

Mean total-pressure losses for the engine air- and bypass-duct flows combined are shown in figure 13. The loss factor $\left(\frac{\overline{\Delta H}_{1b-3,4}}{\overline{H}_{1b}}\right)$ is a true measure of the total-pressure losses between station 1b and stations 3 and 4. The magnitude and trends of the loss curves are, in general, the same as for the engine air duct previously discussed.

Effect of flow control devices on engine air-duct performance.- The effects of control devices on station 2 velocity distributions and engine air-duct total-pressure losses are shown in figure 14 for boundary layer 1. Improvements in velocity distributions were realized in regions adjacent to the diffuser wall opposite the scoop, especially at high bypass flows; however, the improvements were at the expense of the loss coefficient, which more than doubled. Velocity distributions obtained were not sufficiently uniform for practical considerations; also, the vane spacing and locations were found to be critical and the performance would be affected significantly if the inlet-boundary-layer conditions changed.

Methods of Eliminating Model I Design Deficiencies

The model I design, which consisted essentially of a conventional diffuser which was modified by cutting a hole in one wall near the exit

and mounting projecting scoops on the wall, produced a performance which indicates the following basic characteristics:

(1) A scoop projecting into the diffuser produces unsatisfactory performance at low bypass flows due to the high angle of attack on the scoop lip and the rapid expansion caused by the diverging wall on the downstream face of the scoop.

(2) Bypassing appreciable amounts of flow (20 to 35 percent) from one wall of the diffuser produces unsatisfactory performance because the adverse pressure gradients set up by bypassing the flow distort the boundary layer on the opposite wall.

(3) The extended scoops produced appreciable gains in the ram recovery of the bypassed air, especially for distorted upstream-flow distributions.

(4) Some improvements in the engine face velocity distributions are obtainable through use of vanes and vortex generators; however, the investigation indicated that vane placement and alinement were critical.

The adverse characteristics of the model I design could be reduced by bypassing flow from the entire periphery of the diffuser. Such a design would be complicated mechanically and structurally, but would offer no internal aerodynamic problems for the following reasons:

(1) The angle of attack at the scoop leading edge and expansion angle on the back side of the scoop would be automatically reduced because the scoop inlet area would be spread over a longer linear distance.

(2) With appreciable bypass flow, all the boundary layer would be removed by the bypass duct; thus, the engine face velocity distributions would be less affected by adverse pressure gradients set up by bypassing the flow.

Another solution to the problem, which avoids the complexity of bypassing from the entire periphery, consists of using a design similar to model II. The characteristics expected from such a design follow:

(1) The blockage effects of the extended scoop would be eliminated by moving the scoop inlet back to the diffuser exit and increasing the diffuser exit area by the amount of the scoop inlet area; thus, no diffusion would occur in the engine duct downstream from the scoop lip. In fact, model II was designed with a small amount of contraction in the engine air duct to permit the scoop lip to handle high angle-of-attack flow at low bypass flows.

(2) Adverse pressure gradients over and above those of the basic diffuser design would be eliminated except for bypass flows corresponding to bypass-inlet-velocity ratios greater than 1.0.

(3) The bypass ram recovery would be a maximum.

(4) Other factors being equal, the model II designs would require more diffuser length due to increasing the diffuser exit area by an amount equal to the bypass inlet area.

Model II Results

Inlet condition.- Velocity profiles at station 1b are presented for models IIa and IIb in figure 15. The measurements presented were taken in the midplane of the diverging side walls and perpendicular to the vertical plane through the model center for three different boundary-layer conditions. The flow conditions were established in a manner similar to that for model I. For boundary layer 1 for both models the flow was symmetrical with the boundary layer at each wall occupying approximately 30 percent of the duct area. A velocity ratio of approximately 40 was present in proximity to the diffuser walls. The values of Mach number M_{1b} were 0.23 and 0.31 for models IIa and IIb, respectively. For boundary layer 2, the flow was badly distorted by shock—boundary-layer interaction with a low velocity region adjacent to the bypass wall for model IIa and adjacent to the opposite wall for model IIb. A thin boundary layer and high velocity flow existed in proximity to the walls opposite those having low velocity flow. The values of Mach number M_{1b} were 0.34 and 0.43 for models IIa and IIb, respectively. Model center line Mach numbers at station 1b were greater than the M_{1b} values. For boundary layer 3, the flow was again distorted with the low-velocity region on the side of the spoiler, the bypass side for both models IIa and IIb. Similar flow distortions and Mach numbers as for boundary layer 2 were observed. In the case of model IIa, the spoiler was on the diffuser wall from which natural separation occurred, which permitted a comparison of the results with shock—boundary-layer interaction with and without a spoiler. Measurements perpendicular to the parallel diffuser walls indicated symmetrical flow with velocity ratios adjacent to the walls of 0.5 or greater.

Results of total-pressure surveys at station 1b with the scoop installed are presented in figure 16. Data were obtained for both models IIa and IIb for boundary layer 2 for various bypass flows. The total-pressure distribution for model IIa, the model with low-energy air initially on the bypass side, was not significantly affected by the scoop or by bypassing flow. For model IIb, the model with the low-energy air initially on the side opposite the scoop, the presence of the scoop for low bypass flows forced the main flow to lift off the bypass side wall and attach on the opposite wall, thus the scoop significantly affected the distribution as well as the quantity of air bypassed. The distributions for the scoop installed and 30-percent bypass flow and for the

scoop removed are approximately the same. Mass-weighted total pressures for station 1b were not appreciably affected by these changes in distribution.

Longitudinal wall static-pressure distribution.- Static-pressure distributions for model IIa for boundary layers 1 and 2 are presented in figures 17(a) and 17(b), respectively. Since, with no bypass flow, the flow must contract from the full diffuser exit area to the engine duct area, a large pressure-drop coefficient for boundary layer 1 (favorable for producing uniform distributions) of about 1.1 was obtained. As the bypass flow approached design value (32 percent), the pressure coefficient approached zero. Thus, for the range of bypass flows examined, no net pressure rise between stations 1a and 2a was obtained. Distributions for boundary-layer conditions 1 and 2 were similar, but boundary-layer condition 2 produced somewhat less pressure drop (flow acceleration) and a net pressure rise for bypass flows in excess of about 16 percent. Thus, a retarded-velocity region on the bypass side caused the area contraction to be less effective. Data for model IIb, not included herein, followed similar trends and lead to the same general conclusions.

Exit velocity distribution and total-pressure distortions.- Velocity distributions at station 2a are presented in figure 18, and total-pressure distortions at stations 2a and 2b for models IIa and IIb are presented in figure 19. For model IIa and boundary layer 1, the profile for zero bypass flow is symmetrical, the boundary-layer thickness, less than 25 percent of the duct width and the velocity ratio near the walls, greater than 0.80. The distribution was substantially better than at station 1b. Bypassing flow removed the boundary layer on the scoop side; the boundary layer on the opposite wall thickened due to the reduction in favorable pressure gradient (fig. 17) and the velocity near the opposite wall decreased. For 31-percent bypass flow, the distribution was still superior to the distribution at station 1b and vastly improved relative to model I (fig. 9). Distorted flows at station 1b, boundary-layer conditions 2 and 3, had little effect on the distribution at station 2a. Velocity distributions at stations 1b and 2a for boundary layer 2 were similar to those obtained for boundary-layer condition 3, indicating that the presence of the spoiler had little effect. The velocity distributions at station 2a for models IIa and IIb were similar for all three boundary-layer conditions. Even the test condition having distorted flow on the diffuser wall opposite the bypass side (boundary-layer condition 2) did not materially affect station 2a velocity distributions. It is to be concluded from the foregoing discussion that the velocity distributions for model II were vastly superior to those of model I, and that the effects of distorted flows and engine air-duct Mach number level on the distributions were not significant. Further refinements in the bypass-duct design should be possible in applications to specific configurations; for instance, providing a small amount of area contraction on the wall opposite the scoop or favoring the wall opposite the

scoop by accounting for the majority of the required wall divergence with the remaining walls or a combination of both. Velocity distributions at station 2b for the same test conditions as for the data of figure 18 lead to identical conclusions. Velocity distributions were slightly more uniform at station 2b due to natural mixing in the duct section between the two stations.

Several trends are apparent from the total-pressure-distortion data of figure 19. Bypassing flow, distortions of the flow upstream of the scoop, engine air-duct Mach number, and the station of measurement (stations 2a and 2b) all influenced the magnitude of the total-pressure distortions. For example, boundary-layer total-pressure distortions at station 2a were approximately 4 and 7 percent for models IIa and IIb, respectively, as compared with distortions of 8 to 10 percent for model I which was at a lower Mach number level. For distorted flow conditions in the upstream diffuser, model IIa distortions vary from 8 percent at zero bypass flow to 12 percent at 33-percent bypass flow. In a like manner, distortions for model IIb vary from 11 to 18 percent. The distortions for model IIb were higher than for model IIa because of the higher Mach number level in the engine air duct of model IIb. Distortions at station 2b were less than distortions at station 2a for identical upstream conditions because of natural mixing in the short approximately constant-area duct section separating the two stations.

Total-pressure loss.- Figure 20 shows that for model IIa the loss in the engine air and bypass ducts decreased with increasing bypass flow. Reasons for the decrease in loss are the same as for model I discussed previously. The engine air-duct losses were small; loss values for the three test conditions ranged between 0.002 and 0.02 at zero bypass flow and between 0 and -0.04 at 27-percent bypass flow. For reasons discussed previously, data presented in this form may have negative values. The small differences in the velocity profiles at station 1b for boundary-layer condition 2 (natural distorted diffuser flow) and 3 (artificially distorted diffuser flow) were responsible for the small differences in total-pressure loss of the engine air duct for the two conditions. The large variations in bypass duct losses for the three boundary-layer conditions result from large differences in total-pressure levels of air on the bypass side wall of the diffuser. (See fig. 15.)

Losses in total pressure in the engine and bypass ducts for model IIb (fig. 21) are similar to losses in figure 20 for model IIa. Engine air-duct losses were small, ranging for the three boundary-layer conditions from 0.006 to 0.015 at zero bypass to values from 0.02 to -0.03 at approximately 30-percent bypass flow. An exception to the usual trend of decreasing loss with increasing bypass flow is the engine duct loss for boundary layer 2 which increased with increasing bypass flow in the range from 10- to 30-percent bypass. This result was obtained because the total-pressure deficiency was on the diffuser wall opposite the bypass, the

reverse from other test conditions. The loss undoubtedly was also affected by changes in the station 1b total-pressure distribution caused by the scoop and shown on figure 16. These factors would likewise affect bypass-duct losses.

Mean total-pressure losses for the engine and bypass-duct air flows combined are shown on figure 22. These data are a measure of total-pressure losses for the entire flow. The losses for both models IIa and IIb were small, generally less than $1\frac{1}{2}$ percent of the station 1b total pressure, and they represent approximately a 75-percent reduction relative to model 1, scoop 1 (the scoop producing lowest loss). Bypassing air had a favorable effect on losses due to the following factors; a reduction in angle of attack at the scoop lip, the elimination of the dead air and turbulent regions in front of the bypass and scoop, and the elimination of the adverse pressure gradient in the bypass flow in the vicinity of the scoop.

CONCLUSIONS

In connection with the problem of matching inlet and engine air flows, the basic performance characteristics of several types of designs of subsonic diffuser—bypass-duct combinations were determined for bypass flows up to one-third of the total flow. Direct connected duct models were employed with the important effects of supersonic inlet operation (shock—boundary-layer interaction) obtained by positioning normal shocks in the subsonic diffuser. The Mach number level in the engine air duct ranged from approximately 0.2 to 0.8. The following conclusions were derived:

1. A bypass-duct design procedure whereby a hole is cut in one side of a diffuser and a projecting scoop inserted is greatly oversimplified. For such a design, regardless of scoop extension, it was impossible to obtain satisfactory diffuser-exit velocity distributions over the range of bypass flows. Total-pressure losses were also excessive.

2. Extreme adverse pressure gradients downstream from the scoops established by sudden removal of relatively large quantities of air combined with the diverging wall on the downstream face of the scoops were responsible for the performance deficiencies.

3. A bypass arrangement designed to produce at maximum bypass flow a minimum of adverse pressure gradient between the scoop lip and the engine face station produced substantially better performance. Exit velocity distributions were reasonably uniform, and total-pressure losses

of the engine air duct for all test conditions were less than 2 percent of the total pressure.

4. Velocity distributions for the latter design were found to be relatively unaffected by distorted flow obtained by shock—boundary-layer interaction in the upstream diffuser and to be unaffected by changes in the engine air duct Mach number level from 0.27 to 0.81.

Langley Aeronautical Laboratory,
National Advisory Committee for Aeronautics,
Langley Field, Va., October 16, 1956.

REFERENCES

1. Allen, J. L., and Beke, Andrew: Force and Pressure Recovery Characteristics at Supersonic Speeds of a Conical Spike Inlet With Bypasses Discharging in an Axial Direction. NACA RM E52K14, 1953.

2. Beke, Andrew, and Allen, J. L.: Force and Pressure-Recovery Characteristics at Supersonic Speeds of a Conical Nose Inlet With Bypasses Discharging Outward From the Body Axis. NACA RM E52L18a, 1953.

3. Allen, J. L., and Beke, Andrew: Force and Pressure Recovery Characteristics at Supersonic Speeds of a Conical Spike Inlet With a Bypass Discharging From the Top or Bottom of the Diffuser in an Axial Direction. NACA RM E53A29, 1953.

4. Wood, Charles C., and Henry, John R.: Bypass-Duct Design for Use With Supersonic Inlets. NACA RM L55L13a, 1956.

5. Abramovich, G.: Fluid Motion in Curved Channels. From Collection of Reports on Industrial Aerodynamics and Fan-Construction, Rep. No. 211 (text in Russian), Trans. Central Aero-Hydrdyn. Inst. (Moscow), 1935, pp. 97-151.

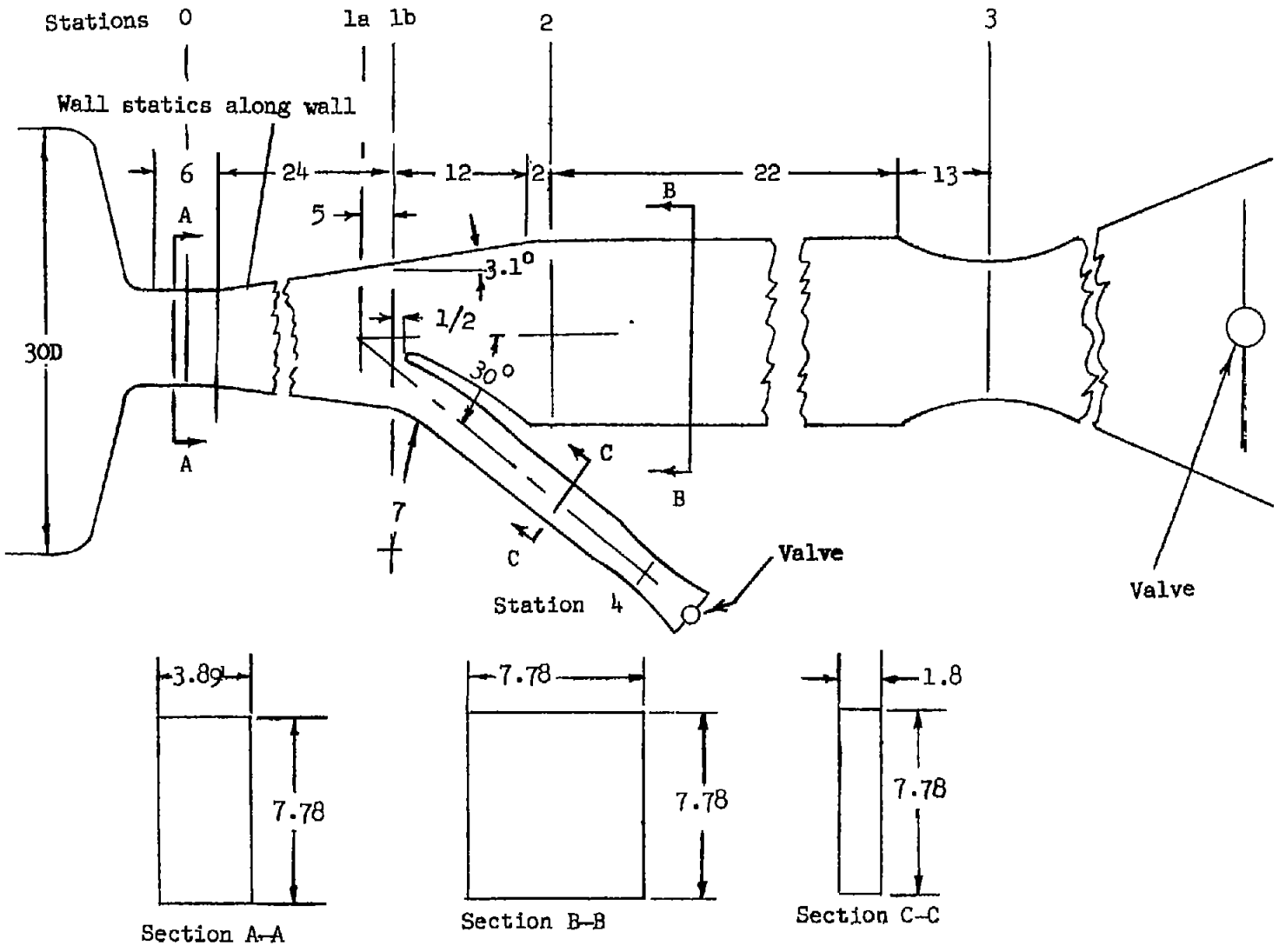

Figure 1.- Schematic diagram of bypass duct configuration I. (All dimensions in inches.)

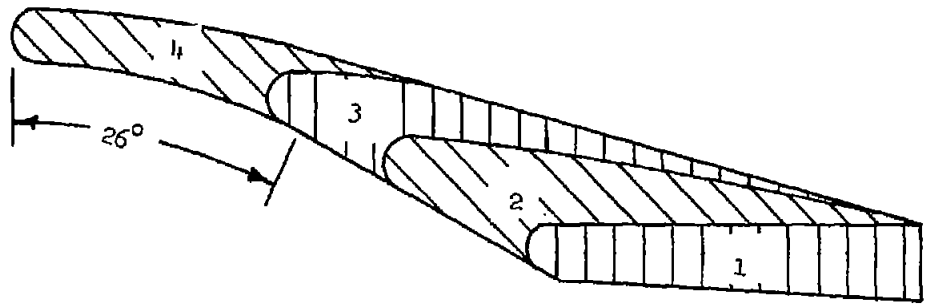

Scoop No.	x	y
1	—	—
2	7.2	10.7
3	8.7	9.8
4	11.85	8.9

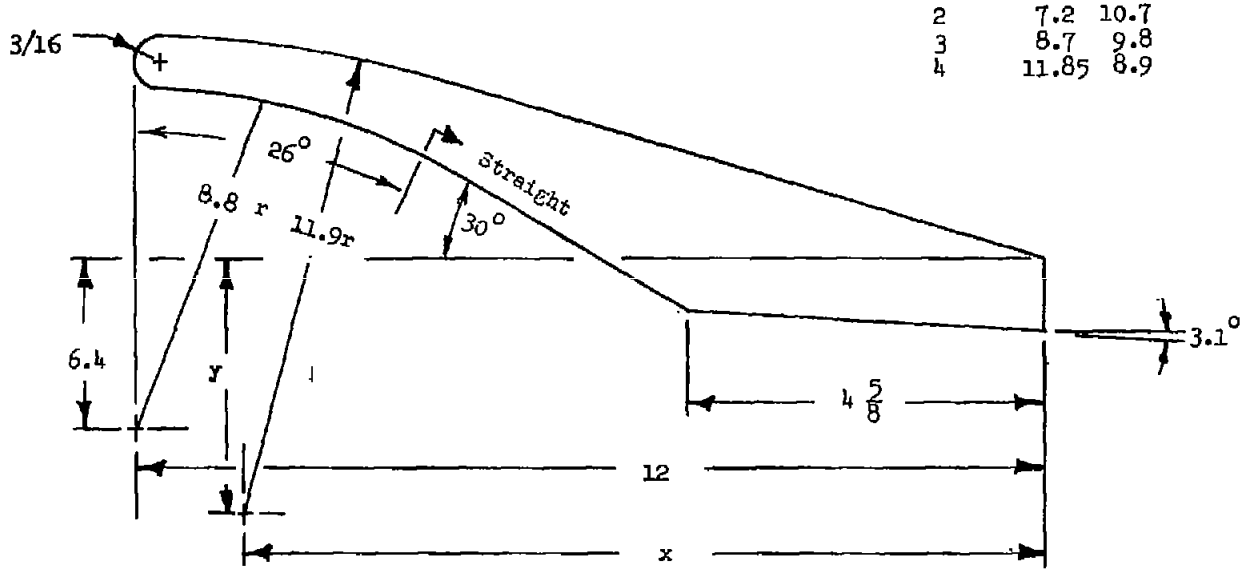

Figure 2.- Diagram of scoops for model I. (All dimensions in inches unless otherwise noted.)

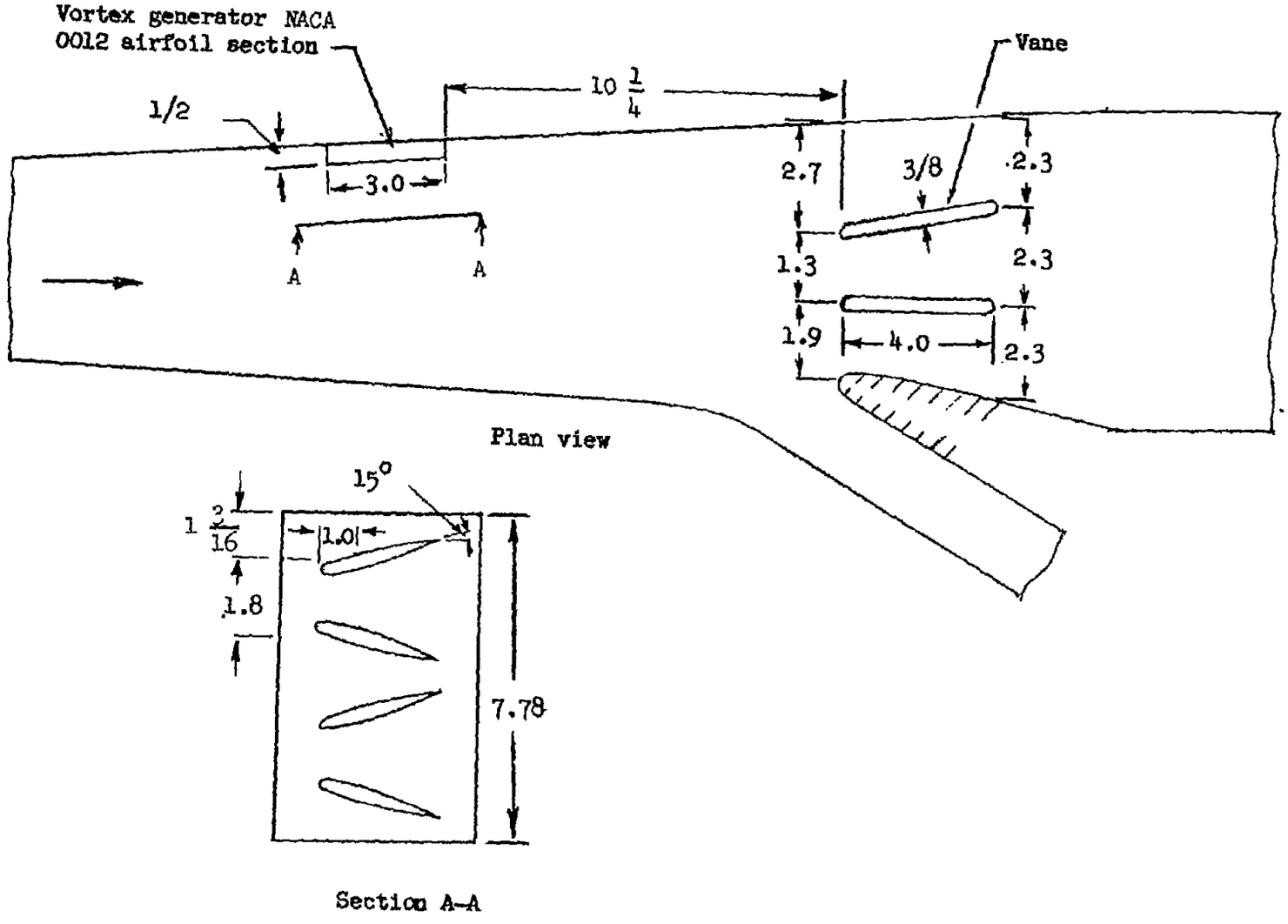

Figure 3.- Diagram of model I showing vanes, vortex generators, and scoop 2. (All dimensions in inches unless otherwise noted.)

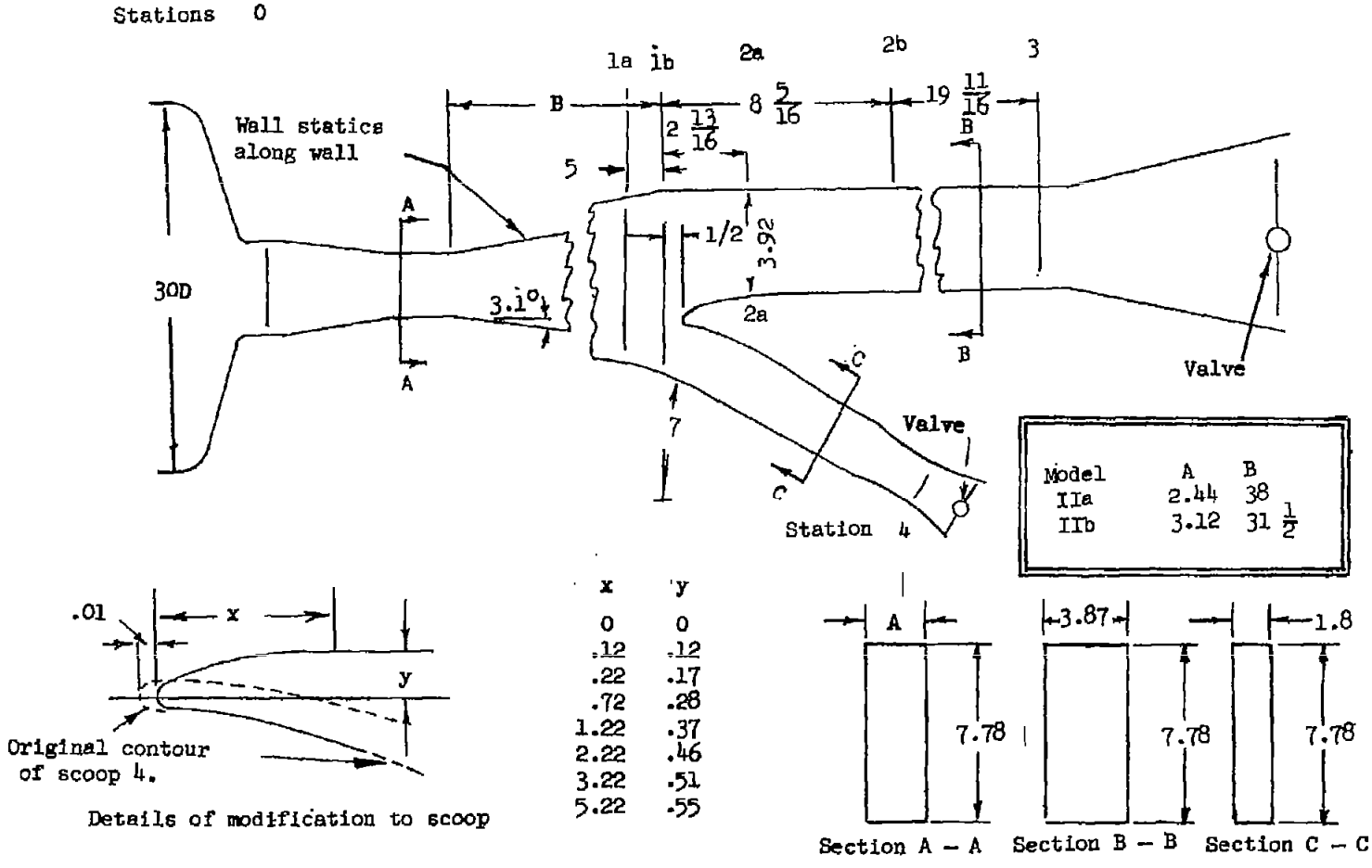

Figure 4.- Schematic diagram of model II. (All dimensions in inches.)

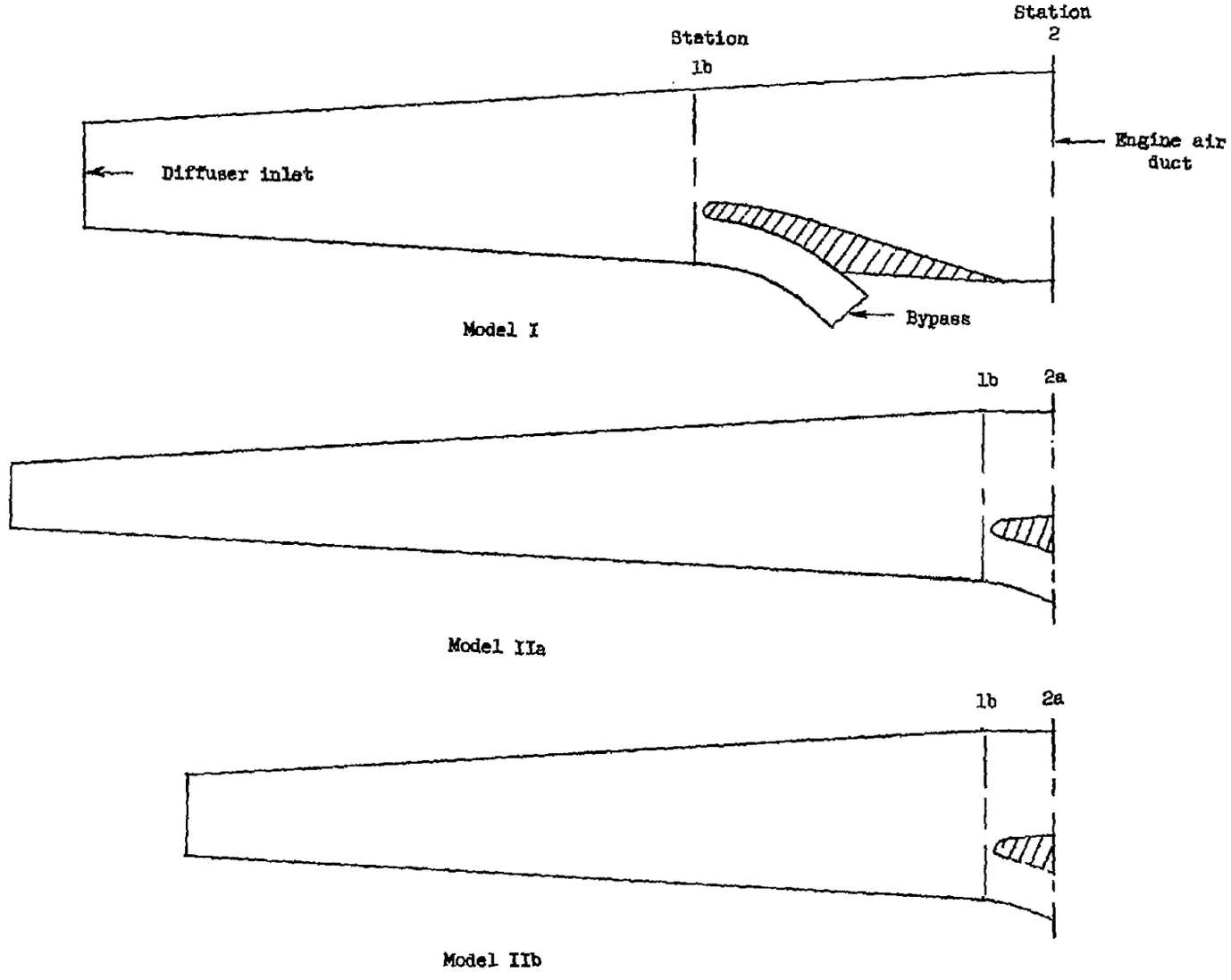

Figure 5.~ Scale drawings of three diffusers tested.

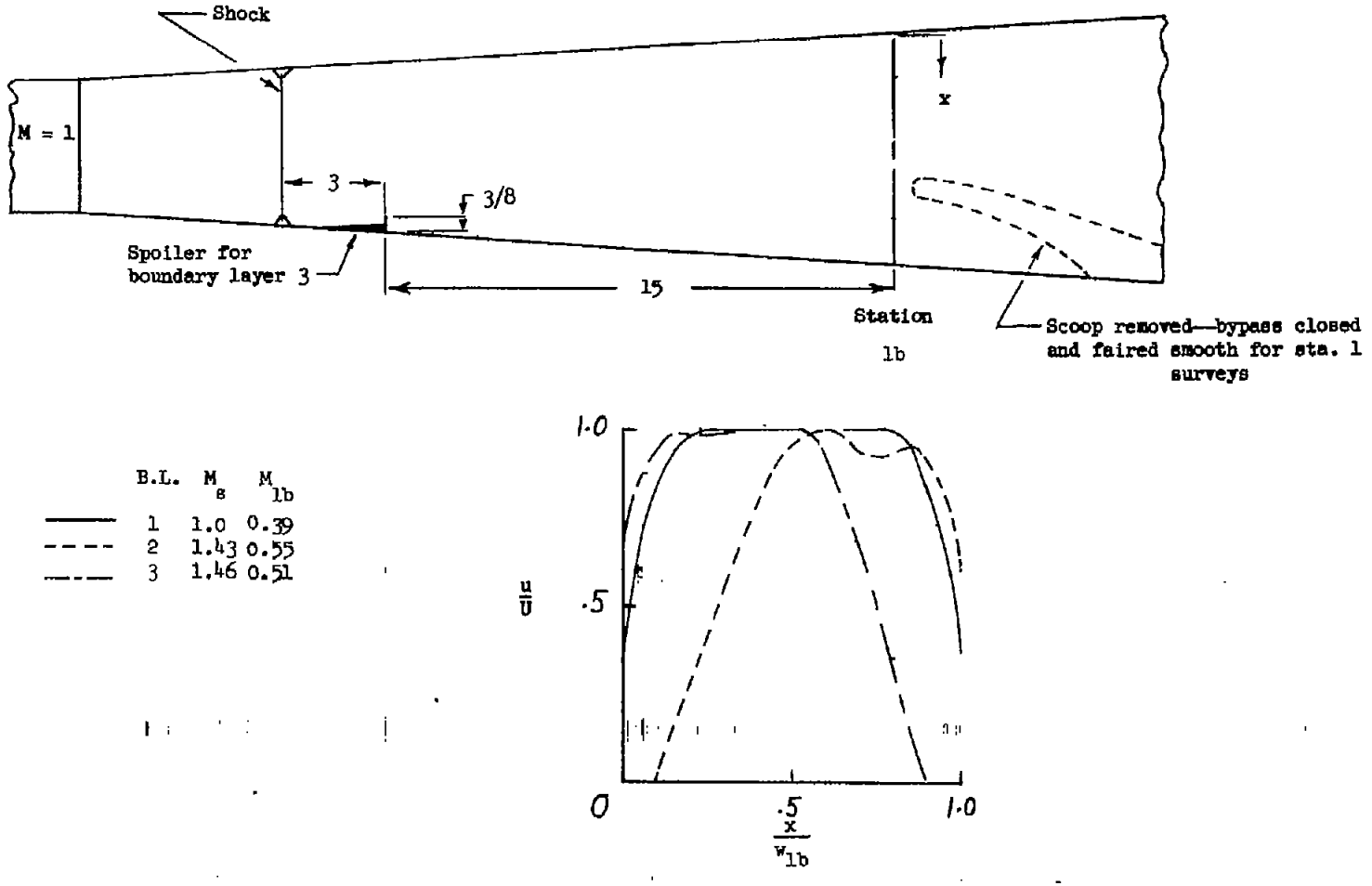

Figure 6.- Velocity profiles at station 1b for test configuration 1.

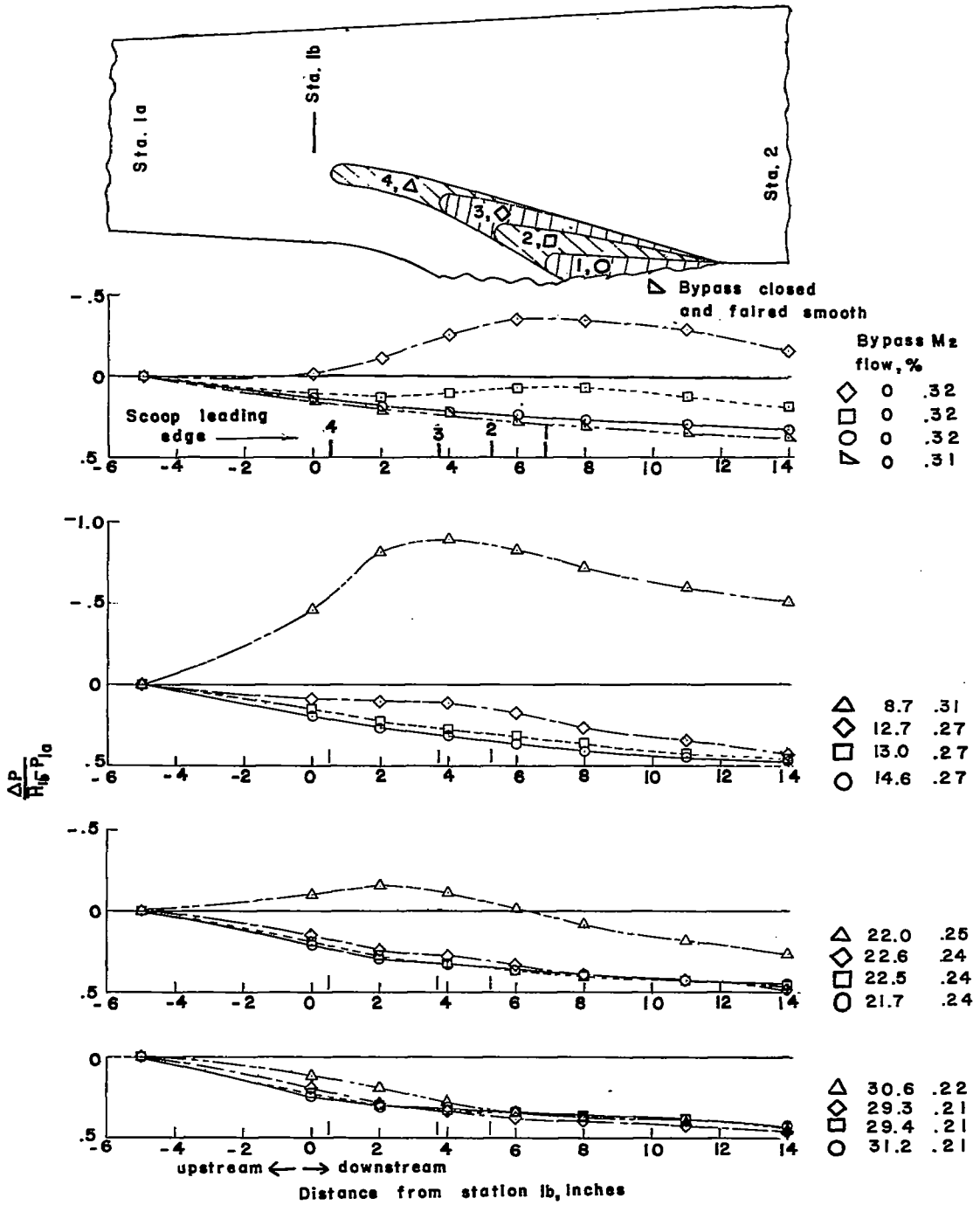

Figure 7.- Static pressure distribution along the diffuser wall opposite the bypass wall for model I. Boundary layer 1.

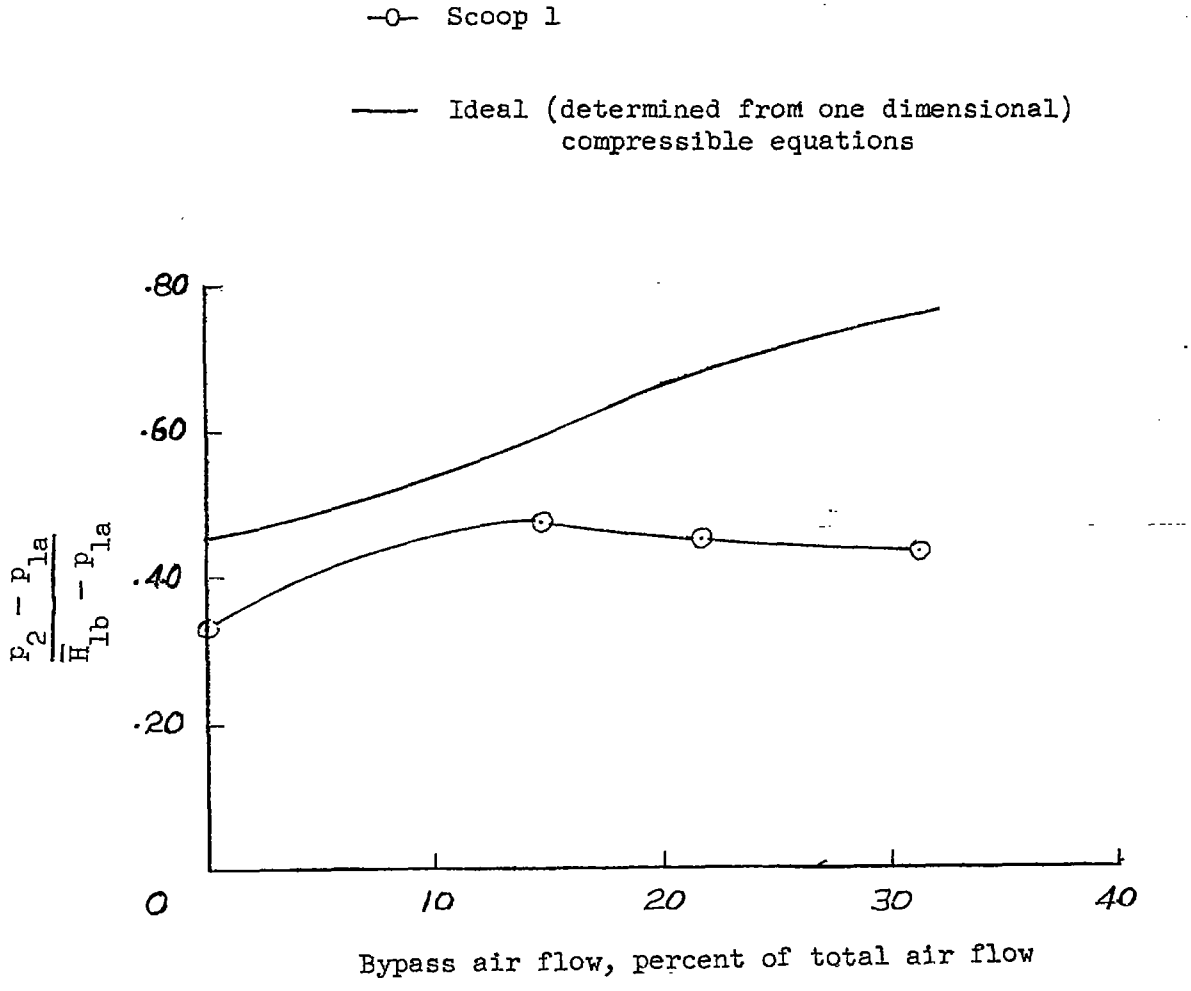

Figure 8.- Comparison of the actual static pressure rise between stations 1a and 2 for boundary-layer condition 1 with the ideal pressure rise. Model I.

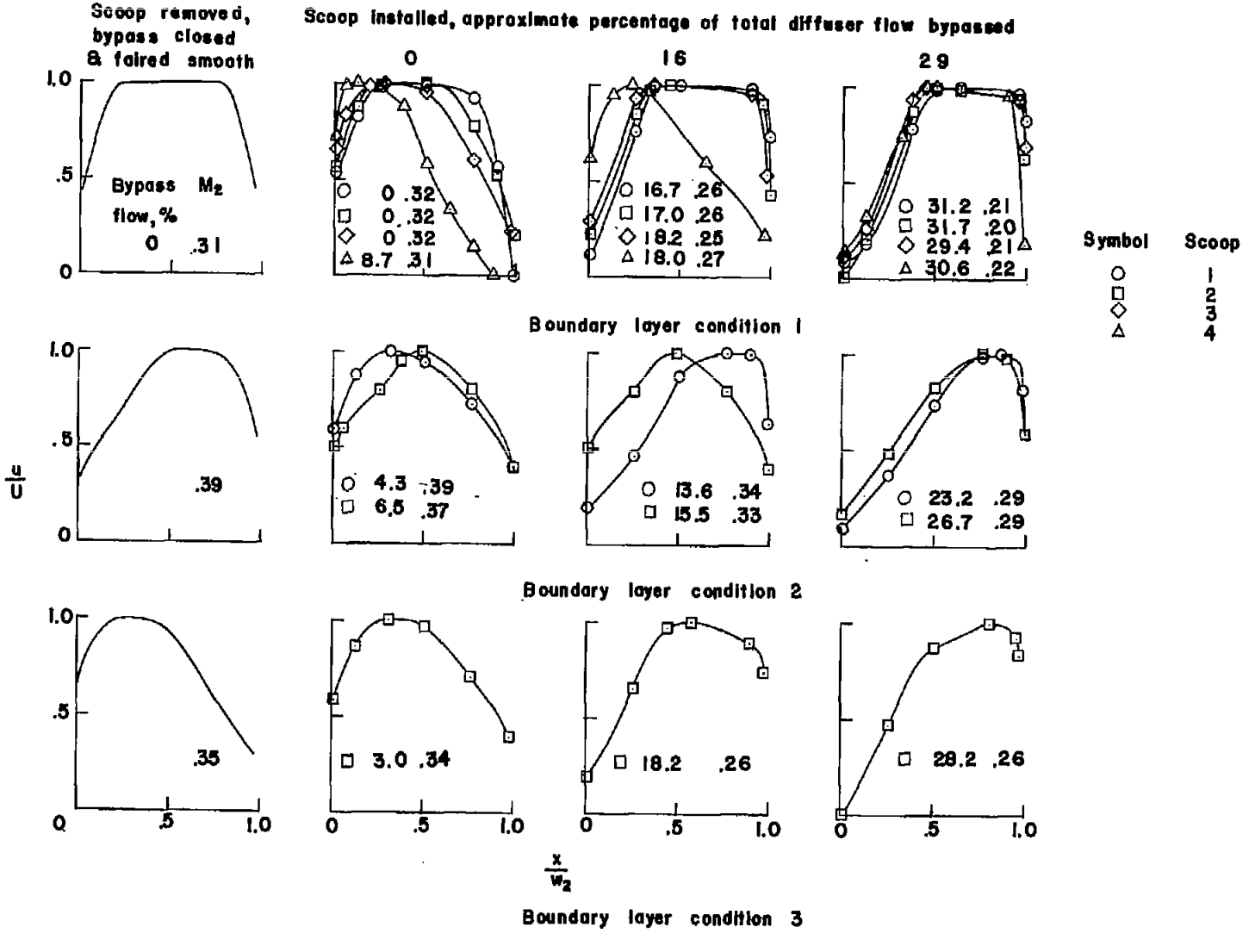

Figure 9.- Velocity distributions at station 2 for model I.

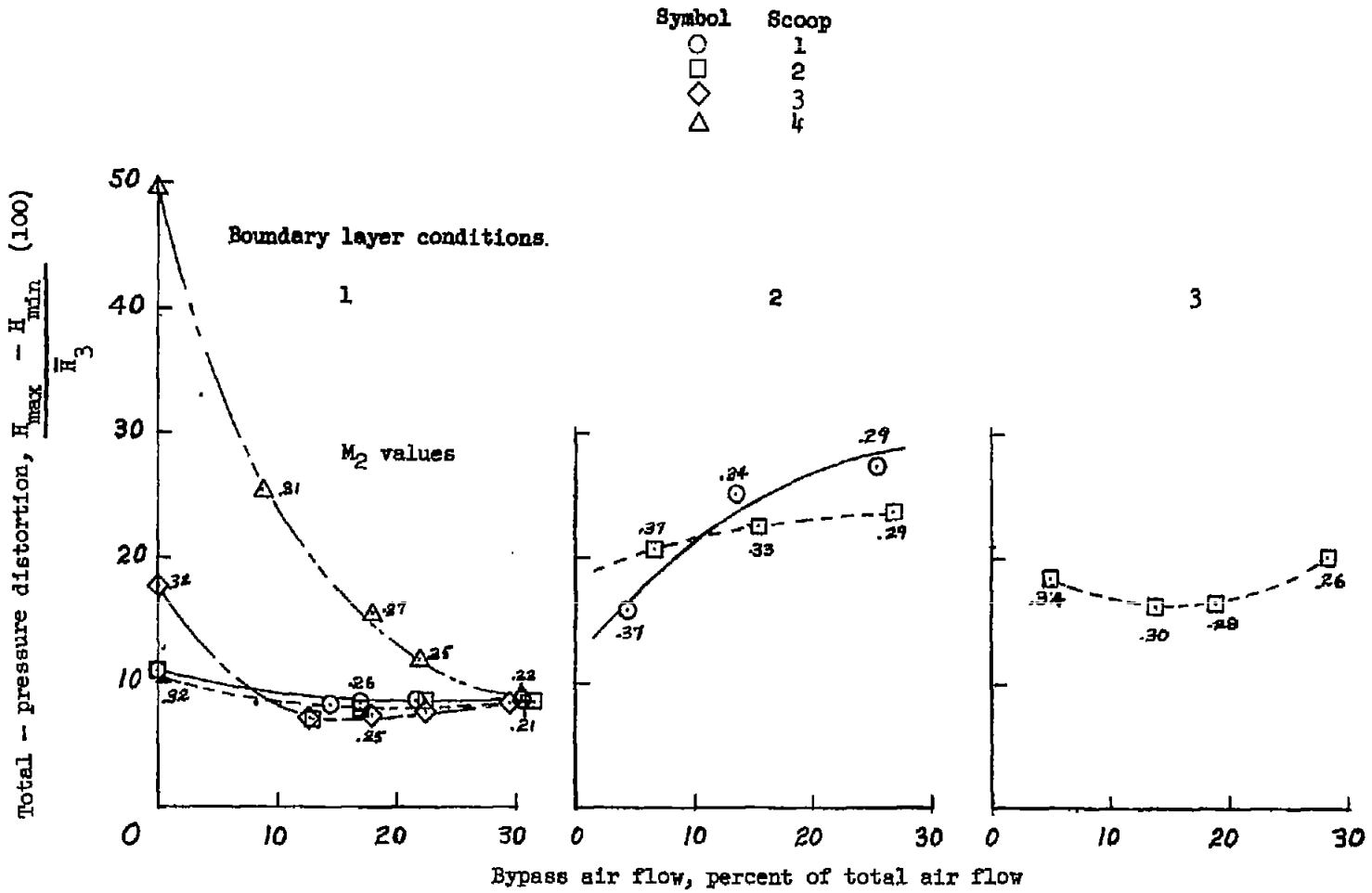

Figure 10.- Total-pressure distortions at station 2 for model I.

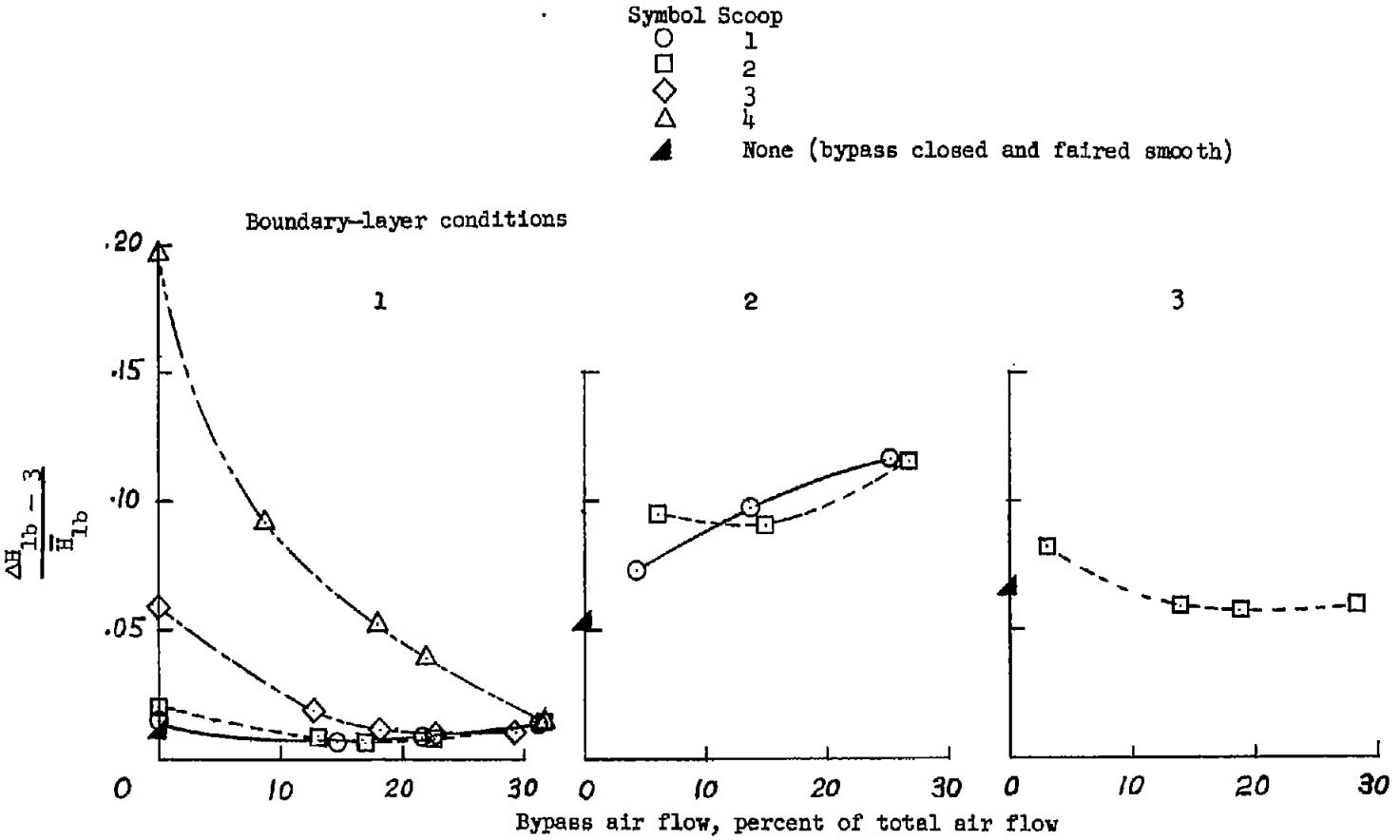

Figure 11.- Total-pressure-loss coefficients for the engine duct. Model I.

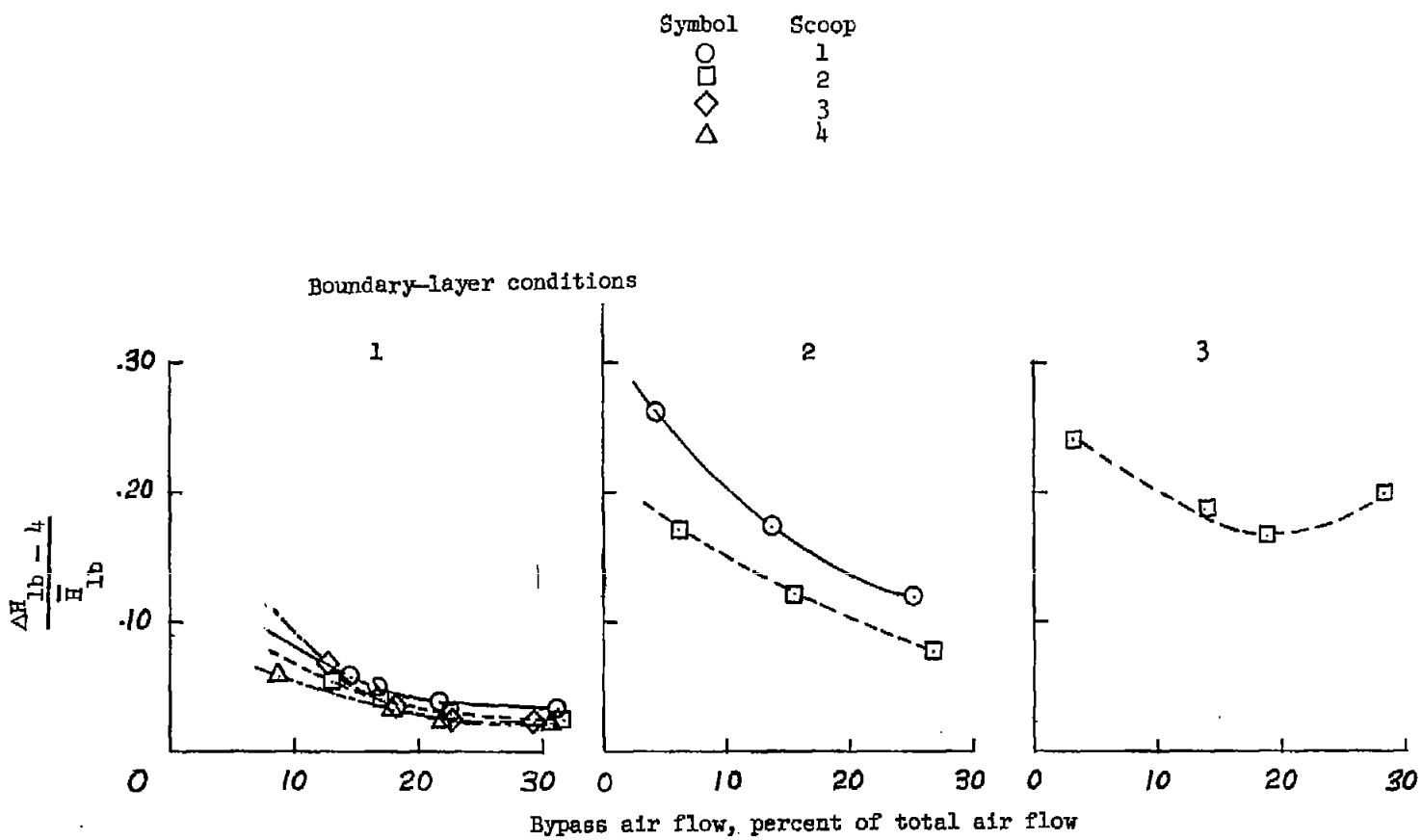

Figure 12.- Total-pressure-loss coefficients for the bypass duct. Model I.

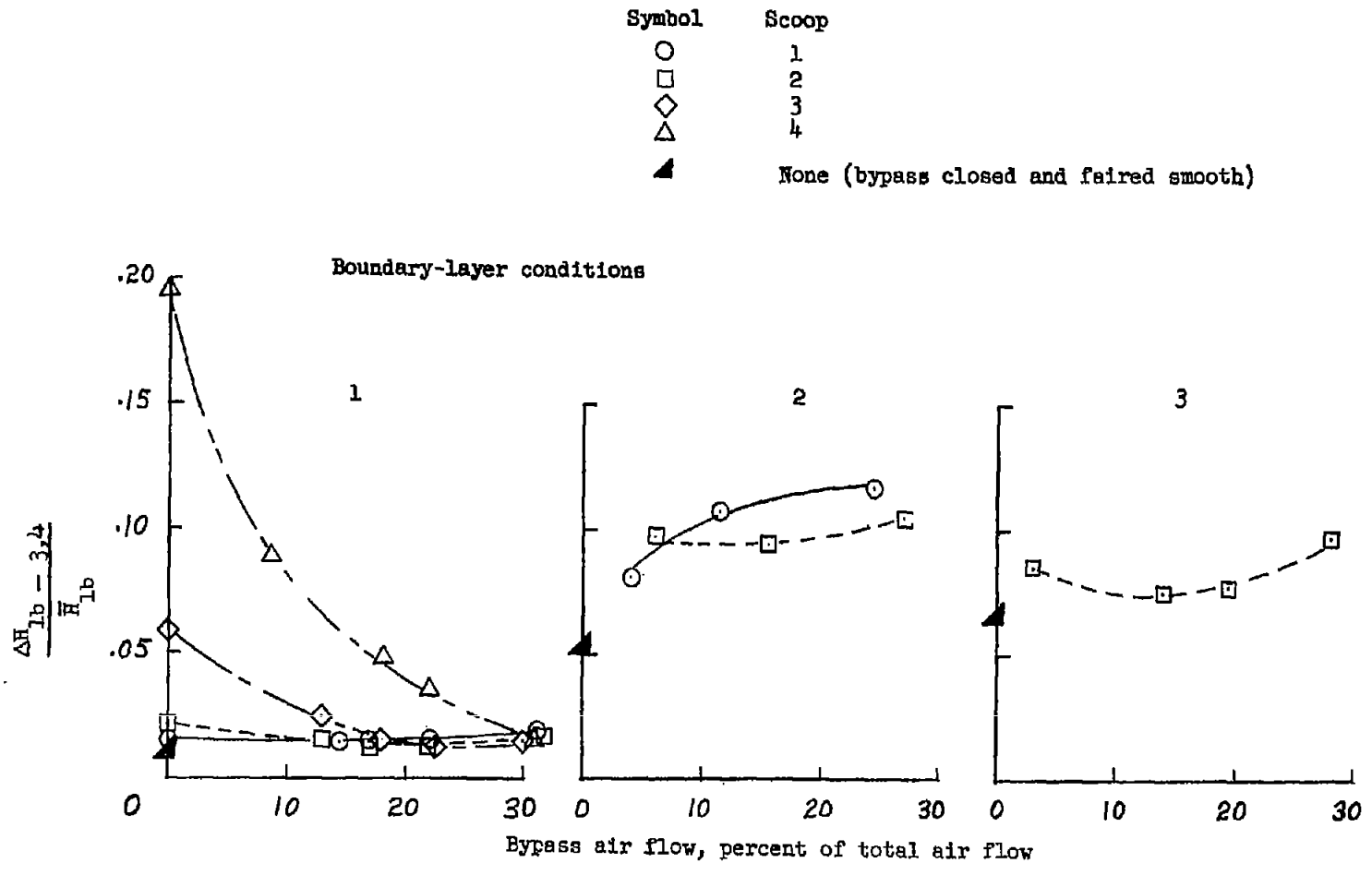

Figure 13.- Mean total-pressure-loss coefficient of engine and bypass ducts for model I.

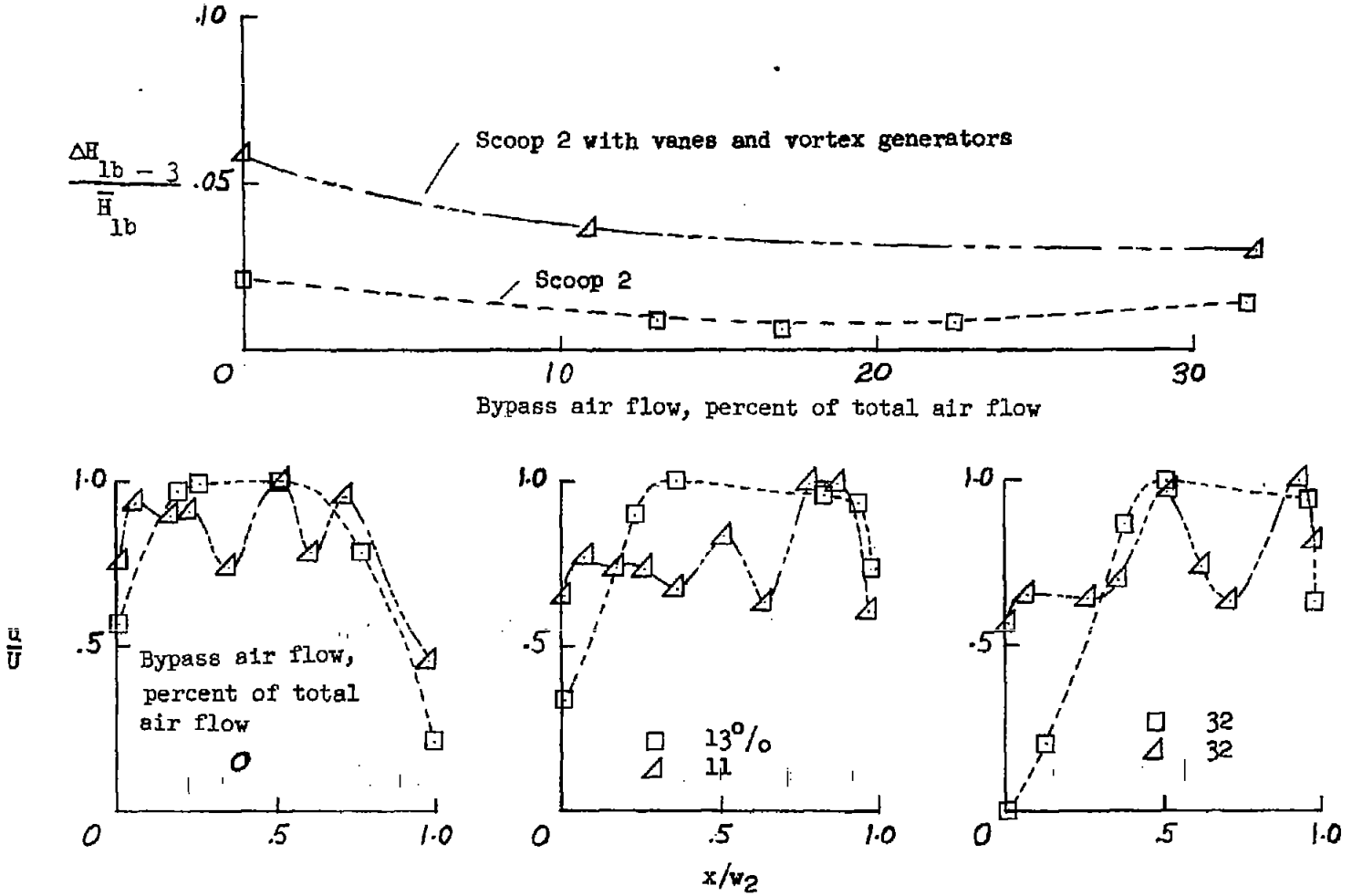

Figure 14.- Effects of vanes and vortex generators on the velocity distribution at station 2 and the total pressure loss in the engine duct for model I.

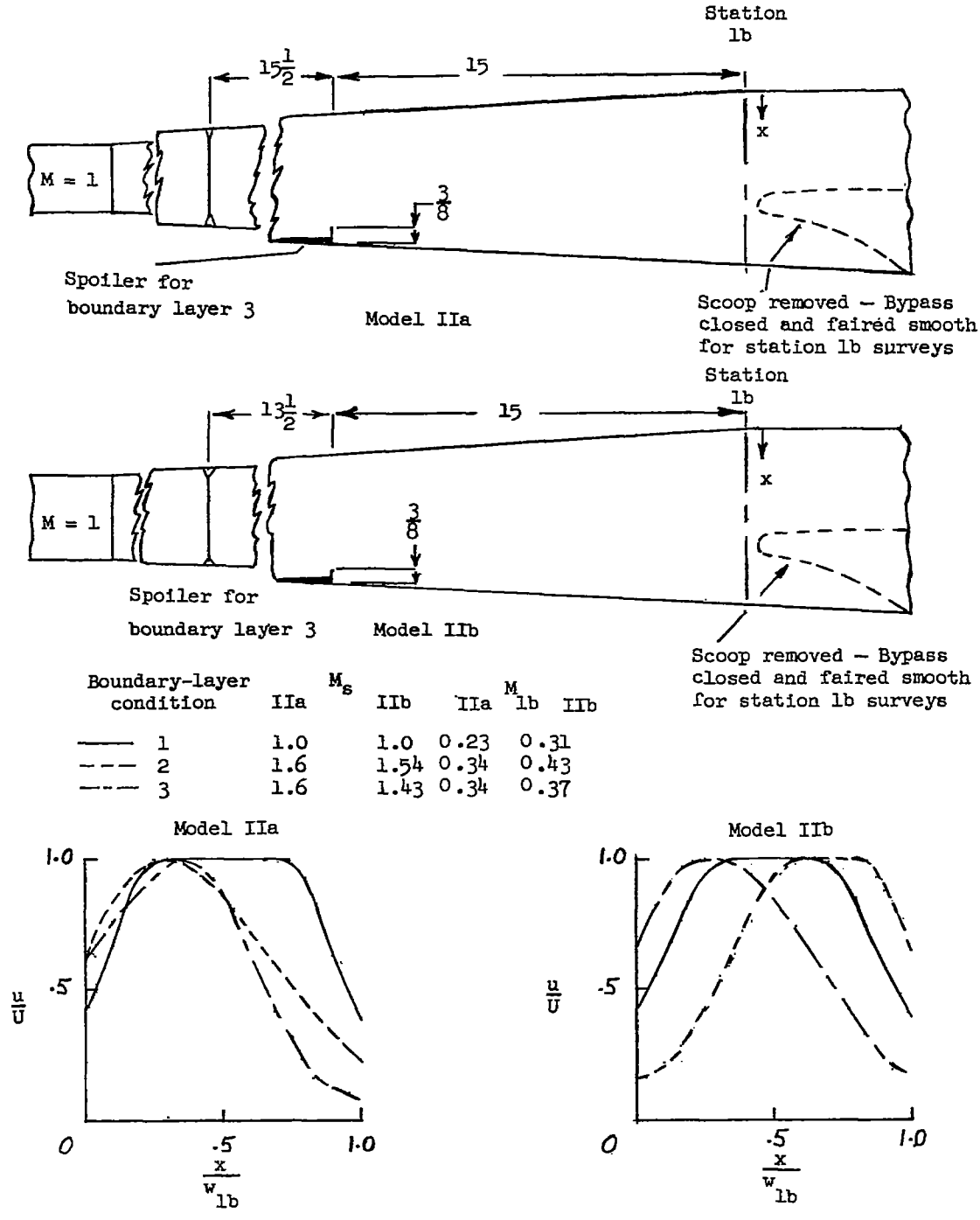

Figure 15.- Velocity profiles at station 1b for models IIa and IIb.

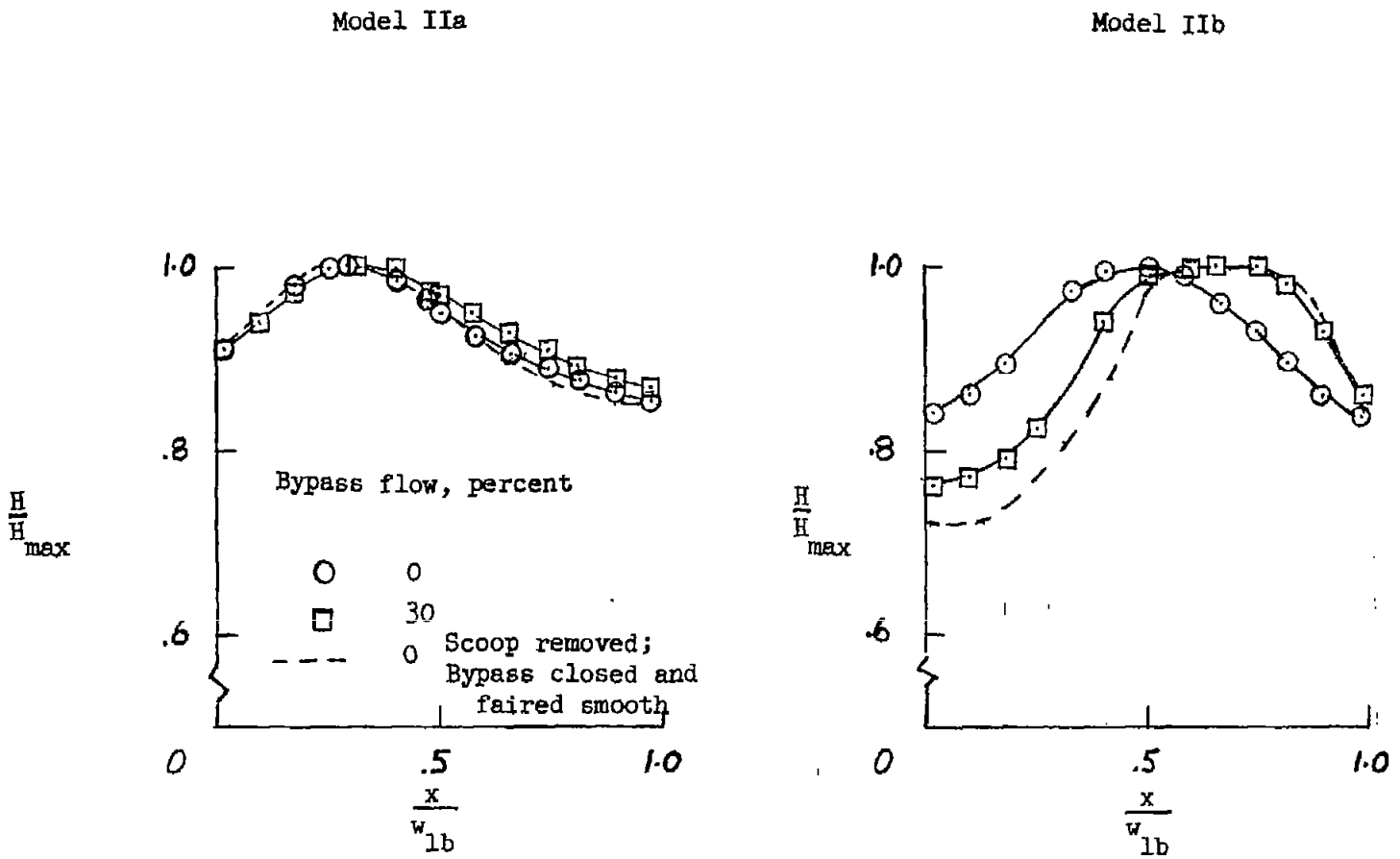

Figure 16.- Effect of the scoop for models IIa and IIb on total-pressure distributions at station 1b for boundary-layer condition 2.

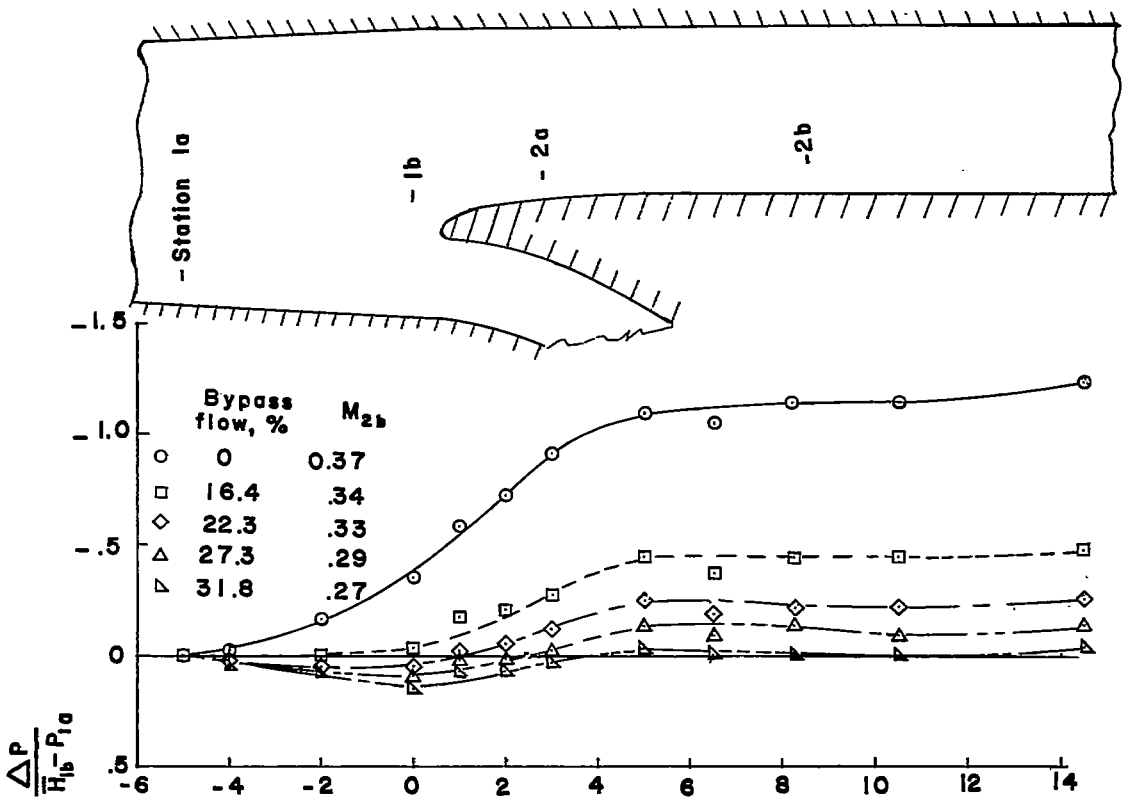

(a) Boundary-layer condition 1.

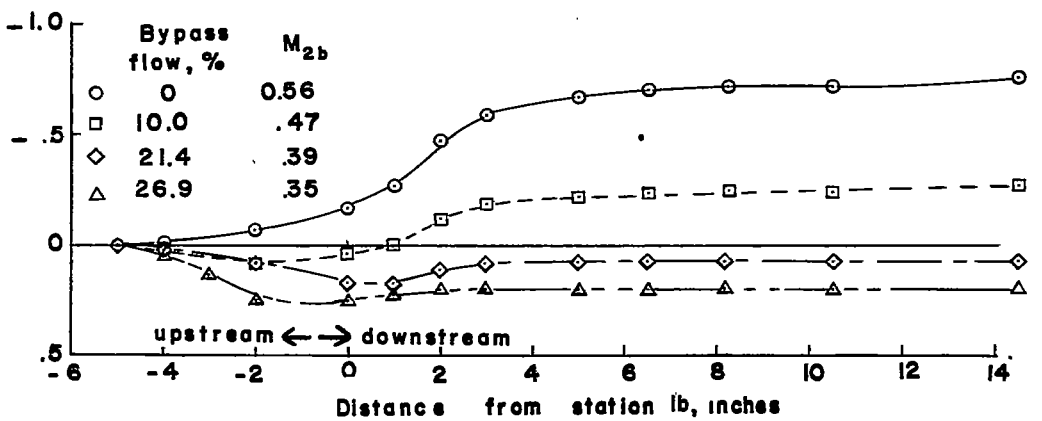

(b) Boundary-layer condition 2.

Figure 17.- Static-pressure distributions along the diffuser wall opposite the bypass for model IIa.

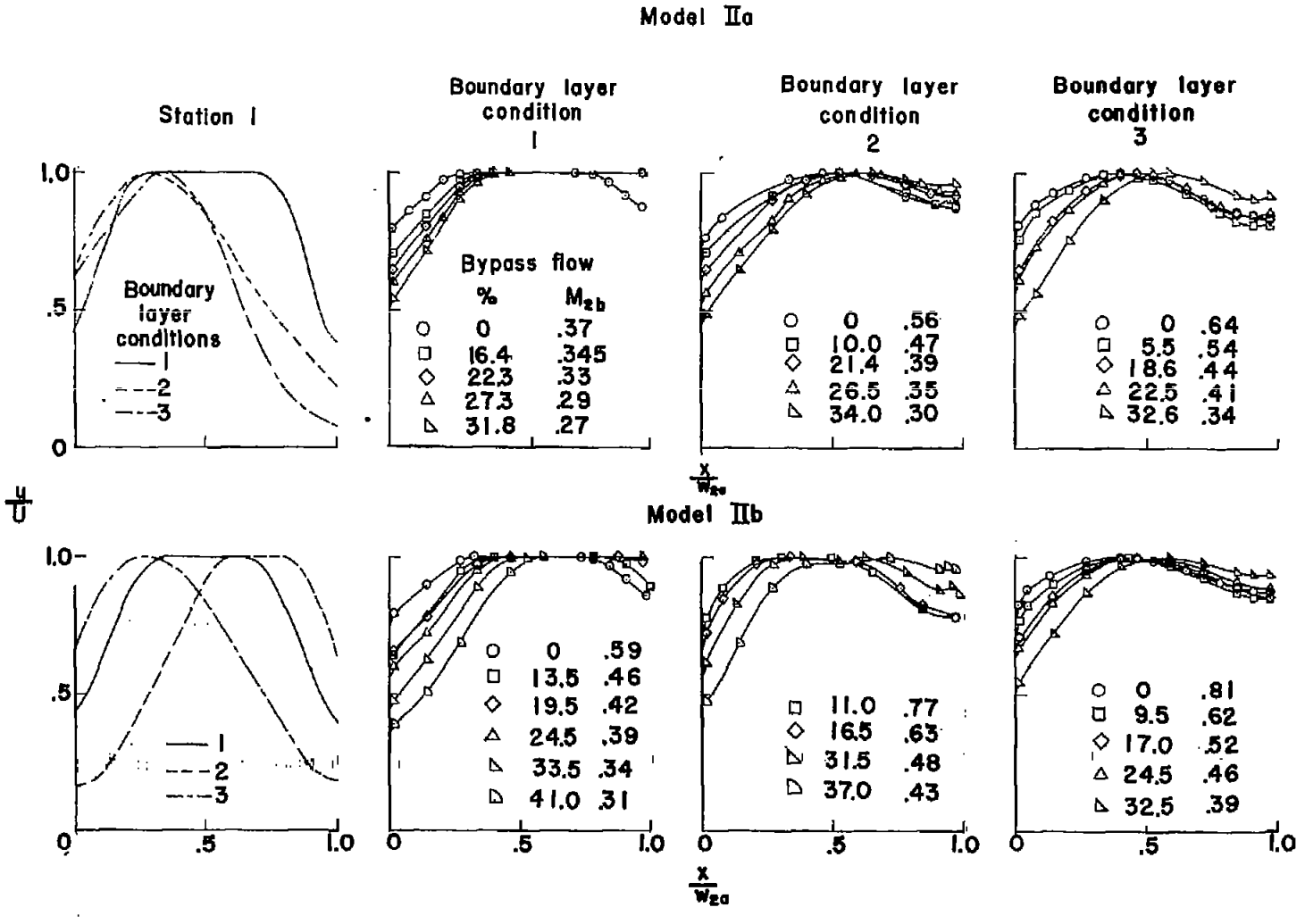

Figure 18.- Velocity profiles at station 2a for models IIa and IIb.

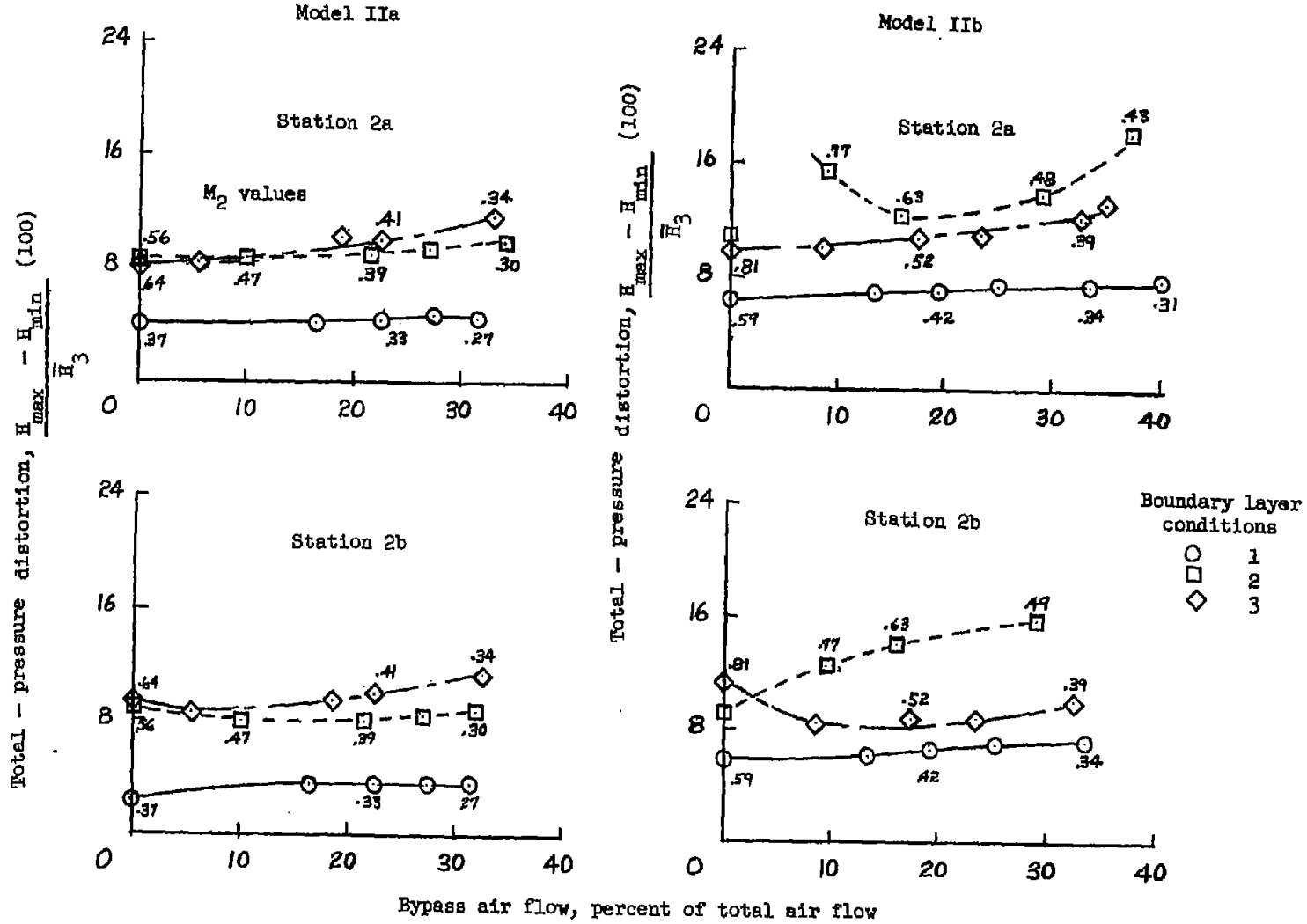

Figure 19.- Total-pressure distortions at station 2 for models IIa and IIb.

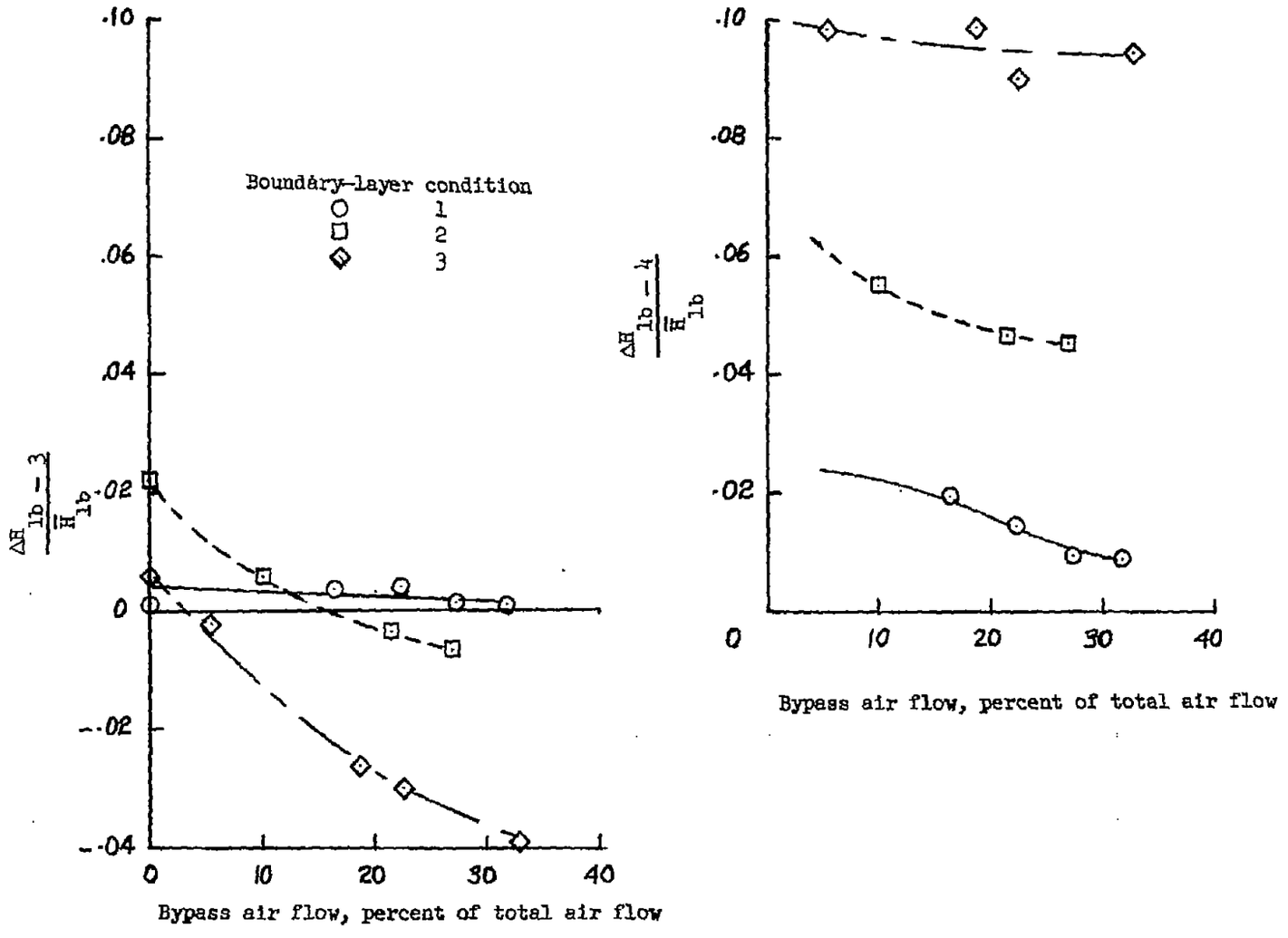

Figure 20.- Total-pressure-loss coefficients in the engine and the bypass ducts. Model IIa.

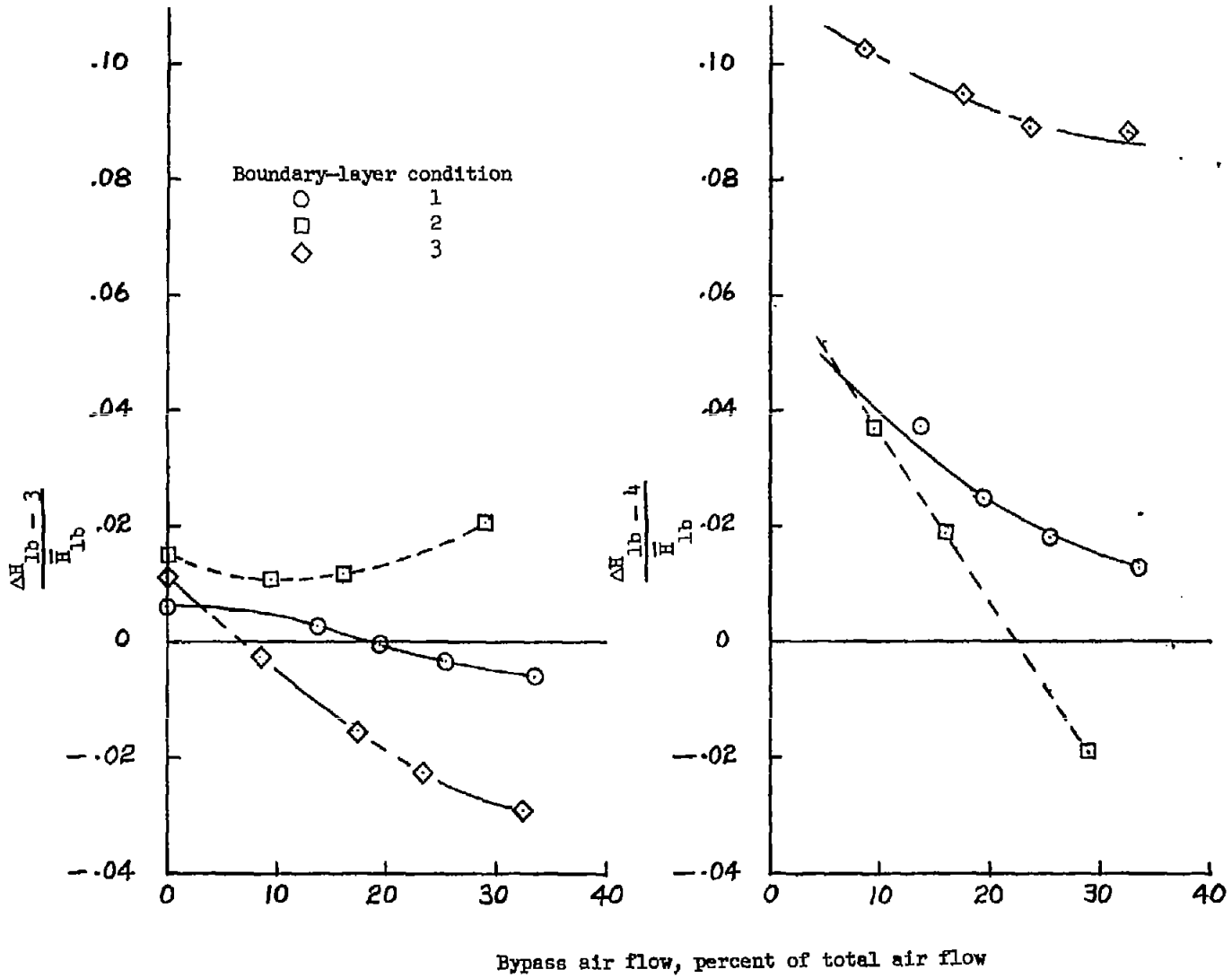

Figure 21.- Total-pressure-loss coefficients in the engine and bypass ducts. Model IIb.

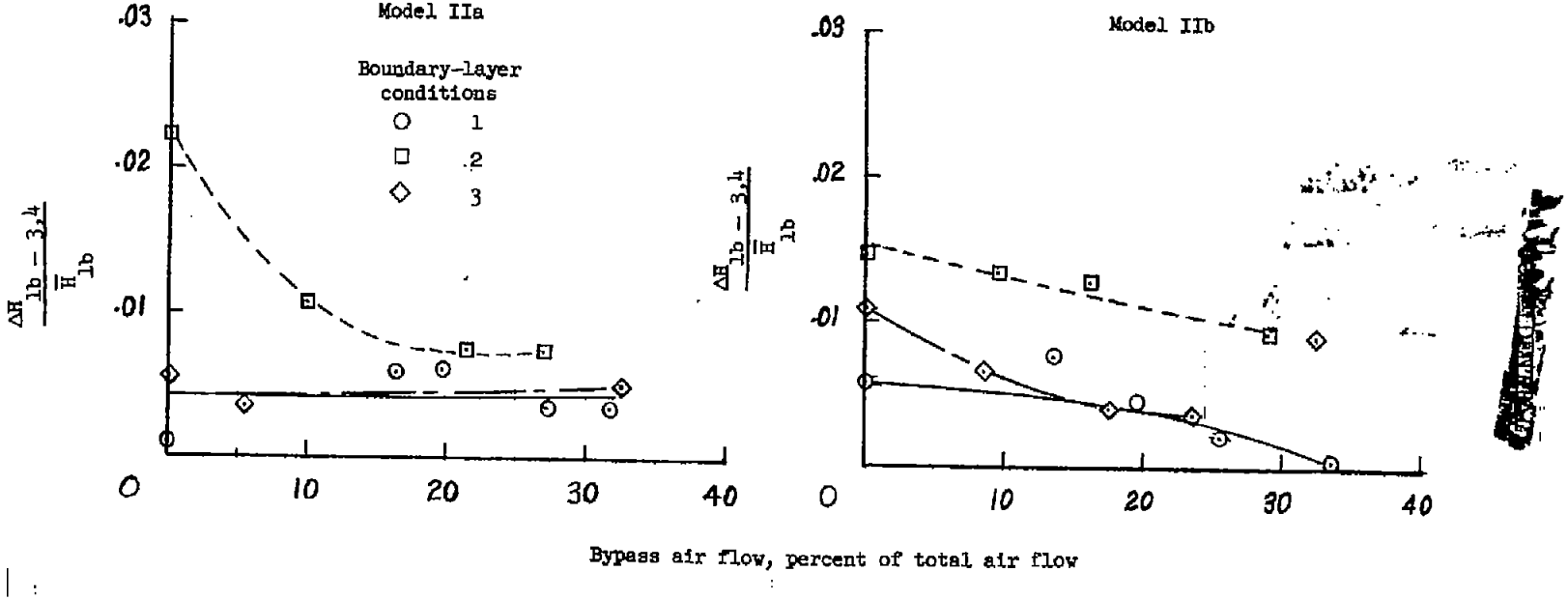

Figure 22.- Mean total-pressure-loss coefficients in the engine and bypass ducts for models IIa and IIb.